https://doi.org/10.5194/egusphere-2025-2234
Preprint. Discussion started: 3 June 2025

An original approach combining biogeochemical signatures and a mixing model to discriminate spatial runoff-generating sources in a peri-urban catchment

Olivier Grandjouan[1#], Flora Branger[1], Matthieu Masson[1], Benoit Cournoyer[2], Nicolas Robinet[3], Pauline Dusseux[4], Angélique Dominguez Lage[2], Marina Coquery[1]

[1] INRAE, UR Riverly, F-69625, Villeurbanne, France
[2] Univ Lyon, UMR Ecologie Microbienne (LEM), Université Claude Bernard Lyon 1, VetAgro Sup, France
[3] UMR CNRS 5194 Pacte, Université Grenoble Alpes, Cermosem, 1064 chemin du Pradel, 07170 Mirabel, France
[4] Institut d'Urbanisation et de Géographie Alpine, Université Grenoble-Alpes, CNRS, PACTE, 38100, Grenoble, France

Correspondence to: Olivier Grandjouan (olivier.grandjouan@insa-lyon.fr)

#: present address: INSA Lyon, DEEP, UR7429, 69621 Villeurbanne, France

Abstract.

Hydrograph separation using biogeochemical data is a commonly used method for the vertical decomposition of flow into surface, subsurface and groundwater contributions. Such approach is not yet widely used for the spatial decomposition of flow. However, it has great potential for estimating contributions linked to specific geological, pedological or land-use characteristics, or to particular anthropogenic contaminant sources, in addition to a vertical decomposition. A mixing model approach was applied to the Ratier peri-urban sub-catchment of the OTHU Yzeron observatory. Eight sources were identified and sampled, corresponding to different land uses (e.g. forest, grassland, breeding), hydrological compartments (e.g. aquifer) and urban point discharges (e.g. sewer system, urban and road surface runoff). A wide range of biogeochemical parameters were analysed including classical (i.e., major chemical compounds, dissolved metals) and innovative tracers (i.e., dissolved organic matter characteristics, microbial indicators). A Bayesian mixing model method was used to decompose streamwater compositions sampled at the outlets of two sub-catchments, under contrasted hydro-meteorological conditions. Results showed distinct biogeochemical signatures mostly linked to the land-use and the geological compartments. The estimated contributions were contrasted and strongly influenced by the hydro-meteorological conditions. The inferred contributions were used to improve an existing perceptual hydrological model of the Ratier and Mercier catchments, at the hillslope scale. This confirmed the potential of biogeochemical data to discriminate spatial runoff-generating sources according to land use, in addition to a more traditional vertical decomposition.

Keywords: runoff-generating sources, fingerprints, spatial decomposition, OTHU, OZCAR, Yzeron

https://doi.org/10.5194/egusphere-2025-2234
Preprint. Discussion started: 3 June 2025

1. Introduction

Peri-urban catchments are characterised by contrasting landscapes that can include natural areas (e.g. forests, moorlands), agricultural areas (e.g. crops, grassland) and urban areas (e.g. residential, commercial or industrial areas). These catchments are under considerable pressure from increasing urbanisation, particularly around large cities (Mejía & Moglen, 2010). Peri-urban landscapes are evolving quickly as natural and agricultural areas are decreasing in favour of urban areas (Jacqueminet et al., 2013). The growing presence of anthropogenic contaminants can alter water pathways and lead to serious deterioration of surface water and groundwater quality.

Sewer overflows are major vectors for a large number of contaminants such as organic matter, organic micropollutants, trace metal elements (e.g. Cu, Ni, Pb, Zn), nutrients or pathogens (Chocat et al., 2001; Lafont et al., 2006; Pozzi et al., 2024; Walsh et al., 2005). Impervious surfaces act as vectors for many contaminants, via rainwater runoff on urban surfaces, such as certain metals (e.g. Cu, Pb, Zn; Charters et al., 2016) or polycyclic aromatic hydrocarbons (Bomboï & Hernandez, 1991), and microbes (Bouchali et al., 2024). Agricultural activities can also bring significant contributions of contaminants in water such as pesticides (Giri & Qiu, 2016), veterinary products (Martins et al., 2019), animal fecal contamination (Marti et al., 2017) or nutrients via fertilization (Penuelas et al., 2023). Small catchments (~10 km²) are particularly sensitive to the degradation of the surface water quality, as they generally consist of streams close to contaminant sources associated with low dilution capacity (Giri & Qiu, 2016). Effective management of water resources and water quality requires precise knowledge of the water pathways and sources in peri-urban catchments (Gonzales et al., 2009). However, identifying runoff-generating sources and estimating their contribution is difficult, as direct measurement of each contribution is almost impossible (Tardy et al., 2004).

Runoff-generating sources are numerous in peri-urban catchments and can be of different kinds due to the diversity of land uses and the presence of artificial elements that divert water such as sewer systems, sewer overflow devices and impervious areas (Birkinshaw et al., 2021; Jankowfsky, 2011). These sources can be defined as hydrological components (e.g. surface runoff, soil water or groundwater flow; Cooper et al., 2000), as specific land uses (e.g. forest, agriculture, urbanized area; Ramon, 2021), or as point contribution (e.g. sewer overflow or wastewater treatment plant outlet; Pozzi et al., 2024). Runoff-generating sources can also be considered as sub-catchments representing a combination of specific geological, pedological and land-use factors (Barthold et al., 2010).

It is now recognised that the biogeochemical composition of water can provide information on the contributions of runoff-generating sources, which cannot be deduced from rainfall-runoff dynamics alone (Birkel & Soulsby, 2015). The use of geochemical signatures through a mixing model is now commonly applied to estimate contributions of runoff-generating sources to streamflow (e.g. Burns et al., 2001; Christophersen et al., 1990; Ladouche et al., 2001; Lamprea & Ruban, 2011; McElmurry et al., 2014). To this day, this approach is often limited to a vertical decomposition of streamflow according to groundwater flow, subsurface flow and surface runoff (Gonzales et al., 2009; Ladouche et al., 2001). However, this method has also a strong potential for spatial decomposition according to runoff-generating sources linked to the geological,

https://doi.org/10.5194/egusphere-2025-2234
Preprint. Discussion started: 3 June 2025

pedological and land use characteristics of the catchment (Nascimento et al., 2023; Liu et al., 2023; Uber et al., 2019). In addition, the use of tracers is often limited to classical geochemical tracers such as stable isotopes, major ions (Singh & Stenger, 2018) or metals (Barthold et al., 2010). Yet many other biogeochemical parameters show potential for discriminating additional sources, such as characteristics of dissolved organic matter (Begum et al., 2023; McElmurry et al., 2014; Sun et al., 2024) or microbial parameters (Colin et al., 2020; Marti et al., 2017).

The objective of the present study is to identify runoff-generating sources linked to both vertical and spatial characteristics of a small peri-urban catchment (e.g. geology, land use), and estimate their contributions to streamwater in contrasted hydro-meteorological conditions. This approach is based on a large biogeochemical dataset including classical and innovative tracers within the application of a mixing model. This method is applied to the Ratier peri-urban catchment, and its nested Mercier sub-catchment, in France, so as to better understand their hydrological behaviour and to identify potential sources of contamination. First, we present the sampling campaigns for runoff-generating sources and streamwater, as well as sample analysis and the construction of the biogeochemical dataset. Second, we describe the biogeochemical signatures of the sources and their contributions to streamwater obtained through the hydrograph separation. Finally, we assess an evaluation of the constructed signatures for each source, as well as a revision of the initial perceptual hydrological model proposed by Grandjouan et al. (2023), to provide a better understanding of the Ratier and Mercier catchments hydrological behaviour.

2. Materials and methods

2.1 Study area: the Ratier catchment

The Ratier catchment is located west of Lyon, in France. It is part of the Yzeron basin and site of the Field Observatory in Urban Hydrology (OTHU; https://www.graie.org/othu/) and the Critical Zone Observatories: Research and Application OZCAR (https://www.ozcar-ri.org/). It covers an area of 19.8 km² and has an altitude ranging between 250 and 780 m. The catchment climate is temperate with mediterranean and continental influences (Gnouma, 2006). The bedrock is predominantly crystalline with gneiss underlying 96% of the total surface (Figure 1.A). The shallower part of the gneiss is fractured and provides low perennial groundwater storage (Delfour et al., 1989) The fractured gneiss gradually changes to a weathered clayous-sandy saprolite layer, which varies from less than 1 m thick in the upper part of the catchment to 10 to 20 m in the valley bottom (Goutaland, 2009). The delimitation between this layer and the thin sandy to loamy soils is not clear (Braud et al., 2011). The soils are associated with low to medium field capacities, with the exception of valley bottoms characterised by high field capacities (Figure 1.B). Downstream of the catchment, the eastern part is covered by colluvium deposits holding a local aquifer (Figure 1.A). This catchment is typically peri-urban with 44% of agricultural areas, 42% of forest and 15% of urban areas (Branger et al., 2013). Field surveys performed by Bétemps (2021) provided information about agricultural activities, which include cereal crop cultures (10% of the catchment area), bovine (10%) and equine breeding (2%) (Figure 1.C). In the urbanized areas, wastewater and rainwater are managed by a combined sewer network and transferred outside the limits of the catchment; however, they can be released in streams during rainstorms via a sewer overflow device located directly

https://doi.org/10.5194/egusphere-2025-2234
Preprint. Discussion started: 3 June 2025

upstream of the Ratier outlet (Figure 1.D). The Mercier stream is a tributary of the Ratier stream with a catchment area of 7.8 km². Its geology consists entirely of gneiss bedrock. Land use is predominantly agriculture (52%) and forest (42%), with a small proportion of urban areas (5%), including therefore less rainwater drainage facilities than the Ratier catchment.

The Pollionnay pluviometric station (Fig. 1.D) records rain and air temperature since 1997. The mean annual precipitation is 750 mm and the mean annual minimum and maximum temperatures are 6.6 and 18.4°C from 2010 to 2022 (Grandjouan, 2024). Two gauging stations located at the outlets of the Mercier and Ratier catchments allow a continuous hydrological monitoring since 2010 and 1997, respectively (Figure 1.D). Hydrological data show a contrasted hydrological regime, with marked low-flow periods between June and September, particularly upstream where runoff is low throughout the year. The Mercier stream is frequently observed to be dry, unlike the Ratier stream, which is continuously supplied by the colluvium aquifer (Grandjouan et al., 2023). According to the rain and discharge data, the response time (i.e., the time elapsed between the peak of rainfall and the corresponding peak in discharge) for the Ratier catchment is around 30 minutes.

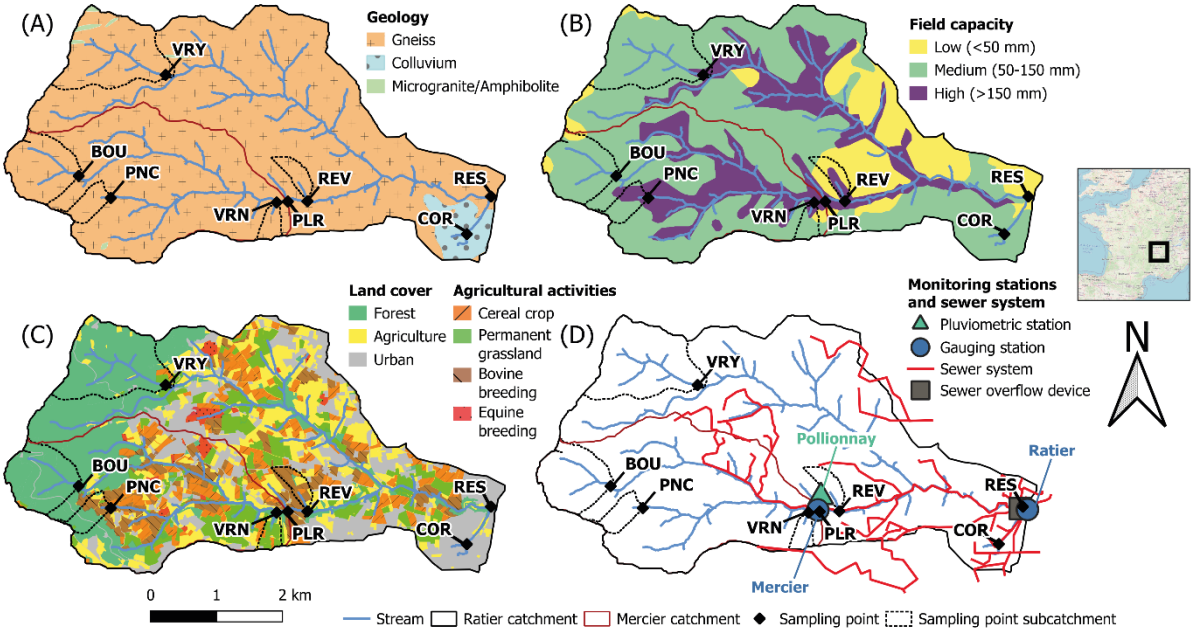

Figure 1 – Maps of the Ratier and Mercier catchments showing the sampling points (see Table 1 for details) and (A) geology (David et al., 1979; Delfour et al., 1989; Gnouma, 2006), (B) field capacity (Labbas, 2014), (C) land use (Jacqueminet et al., 2013) and agricultural activities (Bétemps, 2021) and (D) monitoring stations and sewer system (from Grand Lyon and SIAHVY).

https://doi.org/10.5194/egusphere-2025-2234
Preprint. Discussion started: 3 June 2025

2.2 Field data acquisition

2.2.1 Source identification and sampling

In this study, we consider runoff-generating sources as homogeneous sub-catchments associated with a combination of representative factors including geology, field capacity, land use, agricultural activities, and the sewer. We base our work on the hypothesis that the biogeochemical composition of streamwater at the outlet of these sub-catchments is representative of these factors (Barthold et al., 2010). The first step in identifying these sources involves the superposition of geological, field capacity, land use and agricultural activities maps (Figure 1) to obtain the main combinations of factors existing in the catchment. Sampling points are selected at the outlet of several sub-catchments (Table 1 and Figure 1) according to the predominantly represented combinations of factors and a field reconnaissance to check the consistency of the data, particularly for agricultural activities, which may evolve from year to year. The presence of even a small flow at the sub-catchments outlets is also a requirement for the sampling points selection. The localisation of each sampling point is illustrated in Figure 1. In the case of forest and grassland, two sampling points are selected to compare the biogeochemical signatures obtained from two sub-catchments of the same type (BOU and VRY; VRN and REV). As no homogeneous sub-catchment could be identified for single agricultural activities, an agricultural sub-catchment (PNC) including bovine breeding and cereal crops is preferred. The colluvium groundwater sampling point (COR) is chosen in the upstream section of a stream draining this aquifer. Two distinct runoff-generating sources associated to surface runoff are considered: (1) urban and road surface runoff from impervious areas, and (2) quick surface runoff from other areas resulting from infiltration excess or saturation excess overland flow (Beven, 2012). For the first type of runoff, a stormwater discharge point (PLR) fed by runoff from a road and an upstream urban area is selected. For the second type, sampling of direct surface runoff during rainfall events, from the forest and agricultural sub-catchments (BOU, VRY, REV and PNC) is selected. An additional source is wastewater, which can be transferred from the combined sewer system to the stream through an overflow device located downstream the Ratier catchment (Fig. 1.D), or other overflow pipes. Sampling of wastewater is chosen directly in the sewer system (RES) during periods of rain, to approach a sewer system overflow situation.

https://doi.org/10.5194/egusphere-2025-2234
Preprint. Discussion started: 3 June 2025

Table 1 – Selected sampling points for runoff generating sources and relative sub-catchments areas, geology, field capacity, land use and main features, based on information provided in Figure 1 and field observations.

Sampling point		Sub-basin area (ha)	Geology	Field capacity [1]	Land use (%) and main features					
Site/Source	Code				Forest		Agriculture		Urban	
Bouillon stream	BOU	88	Gneiss	Medium	Deciduous, coniferous	100	-	0	-	0
Verdy stream	VRY	151	Gneiss	Medium	Deciduous, coniferous	100	-	0	-	0
Varennes	VRN	13	Gneiss	Medium	Decidous	30	Grassland	70	-	0
Le Revay	REV	18	Gneiss	Low	Decidous	30	Grassland	70	-	0
Ponce	PNC	28	Gneiss	Medium	-	40	Grassland, bovine breeding, cereal crop	25	Landfill [2]	15
Corlevet spring	COR	-	-	-	-	-	-	-	-	-
Wastewater	RES	-	-	-	-	-	-	-	-	-
Urban and road runoff	PLR	-	-	-	-	-	-	-	-	-
Quick surface runoff		-	-	-		-		-		-

[1] Among low, medium and high field capacities identified by Labbas (2014).
[2] Soils displaced from urban building sites

In order to assess the seasonal variability of the biogeochemical water composition, sources are sampled in contrasted hydro-meteorological conditions. Low flow conditions are considered from June to September, and high flow conditions from October to May. Wet weather conditions are considered when the cumulative rain over 5 days exceeds 3 mm, and dry weather when it is below 3 mm. Eight source sampling campaigns were carried out between February 2022 and March 2023. Four to 5 samples were collected manually in sampling bottles for each sampling point for a total of 38 source samples.

Some observations differed from the information provided in Figure 1. No bovine breeding was observed at REV during the campaigns, whereas cereal crops were observed at PNC. No direct surface runoff was observed during the campaigns at BOU, VRY, VRN and REV; as a consequence, the quick surface runoff source could not be sampled.

2.2.2 Streamwater sampling during hydrological events

We also sampled streamwater at the outlets of the Mercier and Ratier catchments, targeting contrasted hydrological events. To do so, past hydrological events were extracted from the available for years 2011-2021, and analysed following the approach presented by Braud et al. (2018). Seven hydro-meteorological indicators were calculated to characterise the 315 extracted events, namely: duration of rain, cumulative rainfall, total runoff, 5-day cumulative reference evapotranspiration, dry period duration, antecedent precipitation index, and 5-day cumulative rainfall (Figure 2). Based on a Hierarchical Clustering Analysis (HCA), the events were classified according to the indicators. Three classes of hydrological events were identified: small winter events, summer storm events and major events. Figure 2 shows a Principal Component Analysis (PCA) visualisation

https://doi.org/10.5194/egusphere-2025-2234
Preprint. Discussion started: 3 June 2025

of this classification. Major events are defined by high precipitation rate, long duration and high total runoff volume. Summer storm events are characterised by a long dry period before the beginning of the event and high evapotranspiration rate. Small winter events represent the majority of the extracted events (63%) and are characterised by low values for all the indicators. Antecedent precipitation index (API), which corresponds to the sum of daily precipitation weighted according to a multiplying factor (k = 0.8), and the cumulative rainfall 5 days (R5) before the event, did not mark any specific event class. Based on this classification, we defined a sampling objective of two hydrological events by class.

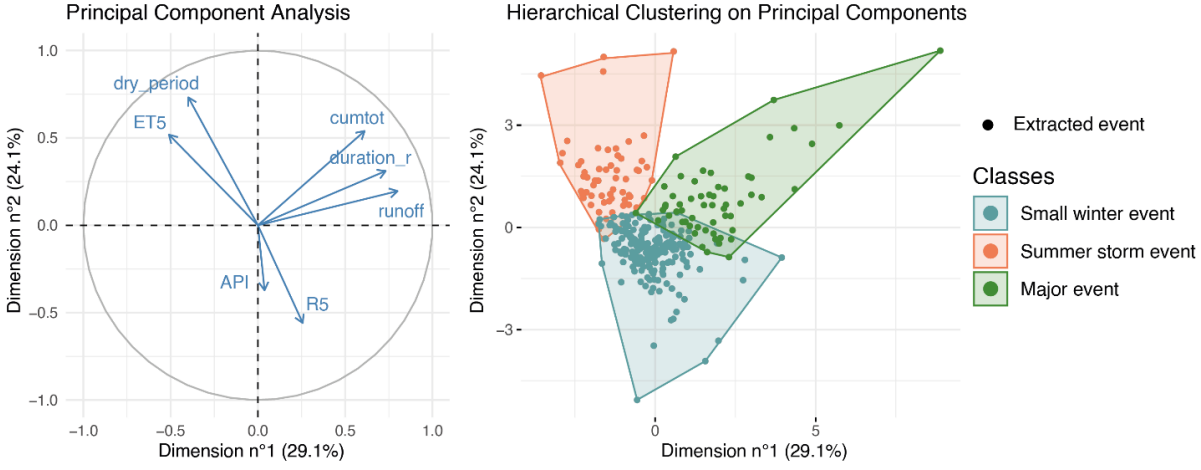

Figure 2 – Principal Component Analysis visualisation of the hydrological event classification based on a Hierarchical Clustering Analysis. duration_r : duration of raining event; cumtot : cumulative rain during the event; runoff : total runoff during the event; ET5 : cumulative reference evapotranspiration 5 days before the event; dry_period : duration of dry period before the event; API : antecedent precipitation index at the beginning of the event; R5 : cumulative rain 5 days before the event.

Automatic samplers (Endress+Hauser Liquiport CSP44) were used to sample streamwater at the Mercier and Ratier gauging stations (Figure 1). A weather alert monitoring was carried out to launch the sampling campaigns according to the targeted hydrological events. Sampling time steps were fixed and adapted to each event, from 10 to 45 minutes, according to the expected duration of the rain. Six hydrological events were sampled between March 2019 and March 2023, ensuring two events per class. Twenty to 24 samples were obtained for each event, and mixed two by two in order to ensure sufficient volume for analysis. After pairing, 10 to 12 samples were finally obtained for each event and at each gauging station. Table 2 shows the hydro-meteorological indicators calculated for these events.

https://doi.org/10.5194/egusphere-2025-2234
Preprint. Discussion started: 3 June 2025

Table 2 – Hydro-meteorological indicators calculated for the hydrological events sampled at the Mercier and Ratier gauging stations. duration_r: duration of raining event; cumtot: cummulative rain during the event; runoff: total runoff during the event; ET5: cumulative reference evapotranspiration 5 days before the event; dry_period: duration of dry period before the event; API: antecedent precipitation index at the beginning of the event; R5: cumulative rain 5 days before the event.

Event sampling campaign	duration_r (h)	cumtot (mm)	runoff (mm)	ET5 (mm)	dry_period (h)	API (mm)	R5 (mm)	Event class
06/03/2019	20	7	0.3	8	55	0	3	Small winter event
10/05/2021	44	92	11.6	13	70	0	10	Major event
03/10/2021	80	89	5.8	13	147	0	0	Major event
22/06/2022	116	57	0.3	38	291	0	0	Summer storm event
14/09/2022	44	9	0.1	15	94	0	2	Summer storm event
13/03/2023	19	18	0.7	7	13	1	27	Small winter event

2.2.3 Streamwater sampling during dry weather

Streamwater composition was also considered at dry weather. Data used come from an available dataset described in Grandjouan et al. (2023). In this latter study, monthly monitoring campaigns were conducted from March 2017 to December 2019 at the outlets of the Mercier and Ratier catchments, and a total of 24 samples were collected manually. These samples were classified into low flow (June to September) and high flow (October to May) conditions.

2.2.4 Sample pre-treatment and analysis

All source and streamwater samples were filtered at 0.45 µm and analysed for a set of 44 biogeochemical parameters including geochemical parameters, characteristics of the dissolved organic matter (DOM), and 8 microbial parameters (Table 3).
Geochemical parameters included 10 major ions, silica and 17 trace metal elements. Major ions were analysed by ion chromatography, silica by colorimetry and trace elements by inductively coupled mass spectrometry (ICP-TQ-MS). The absence of contamination was systematically verified by the analysis of blanks. Limits of quantification (LQ) and analytical uncertainties are detailed in Table A1. The accuracy and uncertainties of the methods were routinely checked using certified standard solutions and reference materials, as well as regular participation in interlaboratory testing.
Characteristics of the DOM included Dissolved Organic Carbon (DOC) and total dissolved nitrogen (DTN) concentrations, 8 Ultra Violet-Visible (UV-Vis) indicators and 7 High Pressure Size Exclusion Chromatography (HPSEC) indicators. The DOC and DTN analyses were performed by high temperature catalytic combustion. The UV-Vis indicators were calculated from absorbance spectra obtained between 200 and 800 nm from UV-Visible spectrophotometry analyses, as described by Li & Hur (2017) and Boukra et al. (2023). The HPSEC analyses were performed as described by Boukra et al. (2023) and HPSEC indicators were calculated from chromatogram obtained with UV detection at a wavelength of 254 nm according to Peuravuori & Pihlaja (1997).

https://doi.org/10.5194/egusphere-2025-2234
Preprint. Discussion started: 3 June 2025

Microbial parameters included 7 microbial DNA targets tracked using a quantitative Polymerase Chain Reaction method (qPCR). The DNA extracts were performed as indicated in Pozzi et al. (2024). The qPCR assays for human (*HF183* DNA target) and ruminant (*rum-2-bac* DNA target) fecal bacterial tracers, and for tracking classes 1 and 2 integrons PCR assays were performed according to Bouchali et al. (2024). Integrons are genetic shuttles that can encode antibiotic resistances, biocide degradation genes, and other functional genes involved in quick adaptive processes (e. g. Colinon et al., 2010).

Table 3 – Measured biogeochemical parameters and respective analytical methods

Parameter family	Biogeochemical parameter	Analytical method
Major anions	Cl^-, NO_3^-, NO_2^-, PO_4^{3-}, SO_4^{2-}	Ionic chromatography NF EN ISO 14911 (1999)
Major cations	Ca^{2+}, K^+, Mg^{2+}, Na^+, NH_4^+	Ionic chromatography NF EN ISO 10304-1 (2009)
Silica	SiO_2	Colorimetry NF T 90-007 (2001)
Dissolved metals	Al, As, B, Ba, Cd, Co, Cr, Cu, Fe, Li, Mn, Mo, Ni, Pb, Rb, Sr, Ti, U, V, Zn	ICP-MS NF T 90-007 (2001)
Dissolved organic carbon and dissolved nitrogen	DOC, DTN	Catalytic combustion NF EN 1484
UV-Visible indicators	E2:E3, E2:E4, E3:E4, E4:E6, S1, S2, SR, SUVA	UV–visible spectroscopy
HPSEC indicators	Mn-254, Mw-254, disp-254, A0-254, A1-254, A2-254, A3-254	High Pressure Size Exclusion Chromatography
Microbial qPCR assays	Total bacteria (G16S), total *Bacteroidales* (BTT), human marker *Bacteroides* (*HF183*), ruminant marker *Bacteroides* (*rum-2-bac*), sewer system marker (*BTS*), classes 1 and 2 integrons	qPCR

2.2.5 Quick surface runoff from non-urban areas

As no surface runoff could be sampled, we consider that the biogeochemical composition of quick surface runoff away from impervious areas is close to the composition of rainwater, assuming that it does not have enough time to acquire significant biogeochemical elements from the soil it flows over. Therefore, this source (SUR) is associated to rainwater biogeochemical composition from the Pollionnay pluviometric station (Figure 1; Lagouy et al., 2022), sampled between 2017 and 2023, for major ions, DOC and UV-Vis indicators ($n = 9$). Data from the Ecully pluviometric station (10 km from Pollionnay) is used for trace metal element concentrations, produced by Dembélé et al. (2008) between 2008 and 2009 ($n = 32$). No data is considered for HPSEC and microbial indicators for the quick surface runoff source.

https://doi.org/10.5194/egusphere-2025-2234
Preprint. Discussion started: 3 June 2025

2.3 Characterization and biogeochemical signatures of runoff-generating sources

2.3.1 Biogeochemical composition and typology of runoff-generating sources

All data obtained from the 38 source water samples and the 52 analysed parameters are used to provide a detailed characterization of the biogeochemical composition for each source. This description is used to compare the biogeochemical composition of the identified sources, as well as to study their variability according to the hydro-meteorological conditions, in order to confirm similarities, and thus the grouping of samples collected from the same type of source (BOU and VRY; VRN and REV) or, on the contrary, the distinction between groups of samples. A Hierarchical Classification Analysis is used to classify the samples according to the biogeochemical dataset and to create a typology of sources. The purpose of this typology is to describe the nature of the sources that will be considered in the mixing model.

2.3.2 Building-up the biogeochemical signatures

A biogeochemical signature can be defined as a limited selection of discriminating and representative tracers, from which it is possible to apply a mixing model approach to estimate the contribution of sources at the catchment outlet. The tracers used in a mixing model must be additive, conservative and discriminating (Christophersen & Hooper, 1992; Tiecher et al., 2015). To build these biogeochemical signatures, we apply a reductionist tracer selection approach based on the biogeochemical dataset for 52 parameters.

All major parameters and metals are considered additives regarding their chemical characteristics (Benjamin, 2014). Non-additive UV-Vis (E2:E3, E2:E4, E3:E4, E4:E6, SUVA, SR) and HPSEC indicators (Mw-254, disp254) are eliminated according to laboratory tests performed by Baduel (2022). Conservative (HF183 and ruminant *Bacteroides* DNA markers) and non-conservative (integrons, 16S rRNA *rrs* gene, *Bacteroidales* DNA marker) bacterial DNA targets are used in this investigation, but their undefined relations with abiotic parameters led to their removal from the parameter list for this particular task. Phosphates (PO_4^{3-}), nitrogen compounds (DTN, NO_3^-, NO_2^-, NH_4^+), Fe and Mn are considered too reactive and therefore non-conservative. Other non-conservative parameters are eliminated by applying a range-test method (Sanisaca et al., 2017; Wilkinson et al., 2013), that check that the concentrations measured in a mixture (here the streamwater sampled at the Mercier and Ratier outlets during the hydrological events) are comprised within the limits represented by the concentrations observed in the source samples. Failure of this test suggests a non-conservative parameter or a missing source (Collins et al., 2017). Non-discriminating parameters are eliminated using a Kruskal-Wallis test (Kruskal & Wallis, 1952) followed by a Dunn post hoc test (Dunn, 1964), with a p-value threshold of 0.05. The null hypothesis is that the distributions of each parameter are identical across all groups; parameter for which this hypothesis could not be rejected are considered non-discriminating. Lastly, the most discriminating tracers are selected using a Linear Discriminant Analysis (LDA) coupled to a Wilks lambda approach (Collins et al., 1997). This method is used to select the smallest combination of tracers showing the highest inter-source variability and the lowest intra-source variability. The remaining tracers are used to build the biogeochemical signatures of the runoff-generating sources.

https://doi.org/10.5194/egusphere-2025-2234
Preprint. Discussion started: 3 June 2025

2.4 Estimation of the source contributions at the outlet of the catchments

A mixing model is applied to decompose streamwater for samples collected at the Ratier and Mercier sub-catchment outlet stations during dry weather, and during the 6 targeted hydrological events. In the absence of rain, urban and road surface runoff, as well as quick surface runoff are not considered as sources contributing to the streamwater samples. We chose a Bayesian approach to resolve the mixing model equations, using the package *MixSIAR* in R (Stock et al., 2018), this approach allowing for the incorporation of uncertainty in both source and mixture data. The prior information chosen for source contributions, representing the initial assumption about the relative contributions of each source, correspond to *1/n*, where *n* is the number of sources considered. The prior information on the biogeochemical parameter concentration for the sources, representing the initial assumption about these concentrations, is modelled as a normal distribution, defined by the mean and covariance matrix of the measured concentration.

3. Results

3.1 Biogeochemical composition and typology of runoff-generating sources

The median and range of concentrations of the biogeochemical parameters measured for the runoff-generating sources are reported in Table A2 for major parameters, Table A3 for metals, Table A4 for the characteristics of DOM, and Table A5 for microbial parameters. These concentrations are illustrated in the form of a heatmap in Figure 3, coupled with a Hierarchical Cluster Analysis on the parameters and sampling points.

The biogeochemical compositions of samples collected from the first forest sub-catchment (BOU) are all clustered together, indicating similar concentrations. Samples collected from the second forest sub-catchment (VRY) do not show clear clustering, showing a variable biogeochemical composition, different from the BOU samples. Samples collected at both grassland sub-catchments (VRN and REV) are well grouped, showing similar compositions, despite their expected differences in terms of field capacity (Figure 1.B). Three of the five samples collected from the agricultural sub-catchment (PNC) are clustered, showing a similar composition, mostly characterised by higher concentrations of As, Co, Mn, Fe. The other two PNC samples are not grouped with the other three, indicating different compositions. Results show a general clustering for the five COR samples representing the colluvium aquifer, marked by significantly higher concentrations for a group of parameters including SiO_2, Li and Ba, in comparison to all other source samples. Among the five samples representing the colluvium aquifer (COR), two showed concentrations higher than 6 $\log_{10}$ number of copies/100 mL of human marker *Bacteroides* (HF183; see concentration range in Table A4), close to the SEW samples concentration, taken directly from wastewater (median 7 $\log_{10}$ number of copies/100 mL). We considered that these samples were contaminated by wastewater, and removed them from the dataset. Wastewater samples (SEW) are also well clustered, showing similar compositions, linked to a large group of parameters comprised of major ions (e.g. Ca^{2+}, PO_4^{3-}), dissolved metals (e.g. Pb, Cu, Zn), DOC, DTN, DOM indicators (A3-

https://doi.org/10.5194/egusphere-2025-2234
Preprint. Discussion started: 3 June 2025

254 and SR) and microbial parameters (e.g. *int1*, *HF183*). The urban and road runoff samples (PLR) show more variability as only two of the four samples are grouped and marked by high concentrations of NO_3^- and V.

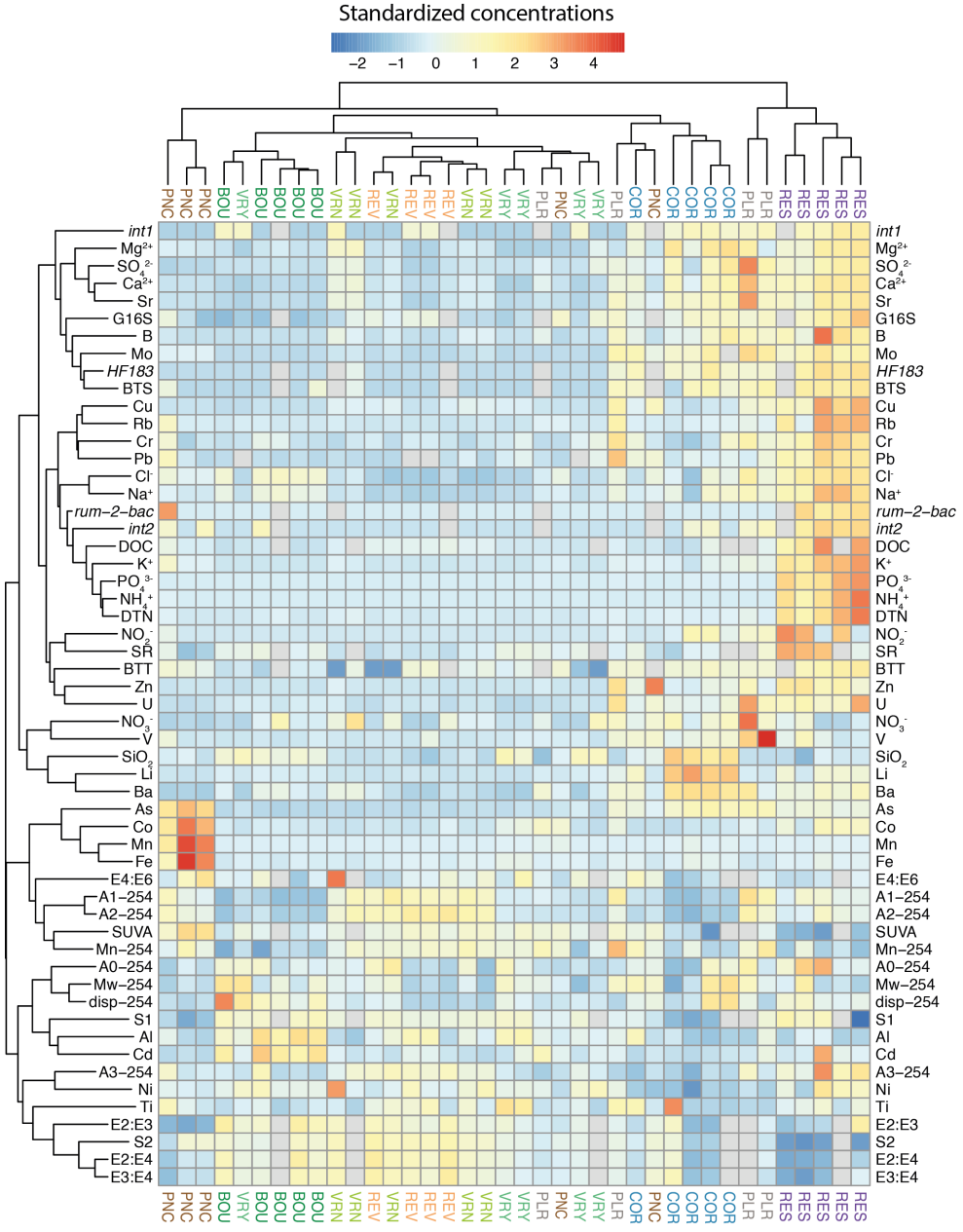

Figure 3 – Heatmap representation of the median concentrations of the biogeochemical parameters in source samples. Standardised concentrations are shown in a range of colours from blue for negative values to red for positive values. Positive values represent high concentrations for a specific parameter and source sample, compared with the other samples. Negative values represent low concentrations for a specific parameter and source sample, compared with the other samples. Biogeochemical parameters and source samples are classified into groups based on Hierarchical Classification Analysis. Quick surface runoff (SUR) was not considered as all biogeochemical parameters were not available for this source.

https://doi.org/10.5194/egusphere-2025-2234
Preprint. Discussion started: 3 June 2025

The differences between the BOU and VRY biogeochemical compositions do not suggest a unique biogeochemical signature associated to forest land use. We thus preferred to consider two different sources related to forest. In contrast, we considered a single source associated to the presence of grassland, based on the clustering of the VRN and REV samples. Each of the remaining sampling points was considered as a distinct source. Table 4 shows the final typology proposed to describe the runoff-generating sources and used for the next step of our study, including the new codes used to describe the nature of each source (FOR-1, FOR-2, GRA, AGR, AQU, SEW, URB and SUR).

Table 4 – Typology of the runoff-generating sources describing the nature of the sources that will be used for the creation of the biogeochemical signatures and in the mixing model (source and colours codes are used thereafter in this study).

Sampling point	Source	Source code	Source color code
BOU	Gneiss – Medium field capacity – Forest n°1	FOR-1	
VRY	Gneiss – Medium field capacity – Forest n°2	FOR-2	
VRN / REV	Gneiss – Low/Medium field capacity – Grassland	GRA	
PNC	Gneiss – Medium field capacity – Agriculture	AGR	
COR	Colluvium aquifer	AQU	
RES	Sewer system	SEW	
PLR	Urban and road surface runoff	URB	
SUR	Quick surface runoff	SUR	

3.2 Building-up the biogeochemical signatures

After discarding the parameters considered to be non-additive and non-conservative according to their nature, 33 parameters remained. Application of the range-test pointed out 13 other non-conservative parameters with concentrations or values outside the range observed for the source samples, mostly concerning the HPSEC indicators and the dissolved metals Al and Co. The Kruskal-Wallis and Dunn tests showed two non-discriminant parameters: Ni and Ti with respective *p-values* of 0.06 and 0.93. Finally, the application of the LDA-Wilks lambda approach (Figure 4) showed that an optimal selection of 15 tracers was sufficient to discriminate the 8 sources. These tracers correspond to 7 major parameters (Cl^-, SO_4^{2-}, Ca^{2+}, Na^{2+}, K^+, Mg^{2+}), 6 dissolved metals (As, Ba, Cr, Li, Rb, Sr), and two DOM characteristics (DOC, spectral slope S2). These parameters were used to build the biogeochemical signatures of each source, represented in the form of radarplots in Figure 5.

https://doi.org/10.5194/egusphere-2025-2234
Preprint. Discussion started: 3 June 2025

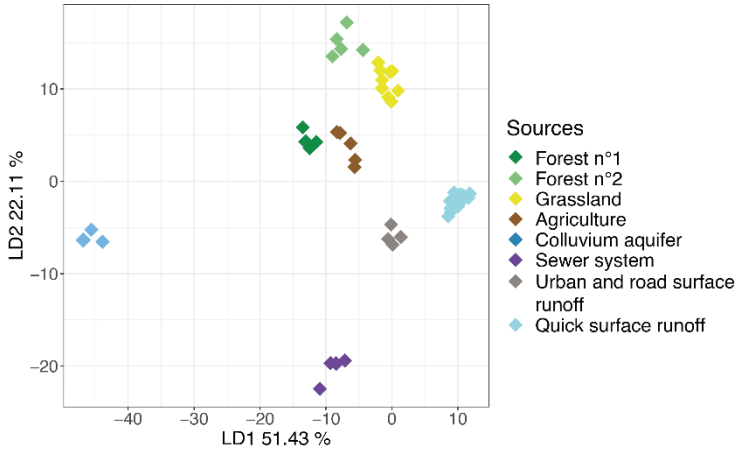

309

310 **Figure 4 – Source samples coloured according to the sources identified and projected along the axes created by the Linear**
311 **Discriminant Analysis. The concentrations used correspond to the optimal selection of tracers resulting from the selection by**
312 **minimisation of Wilks' lambda.**

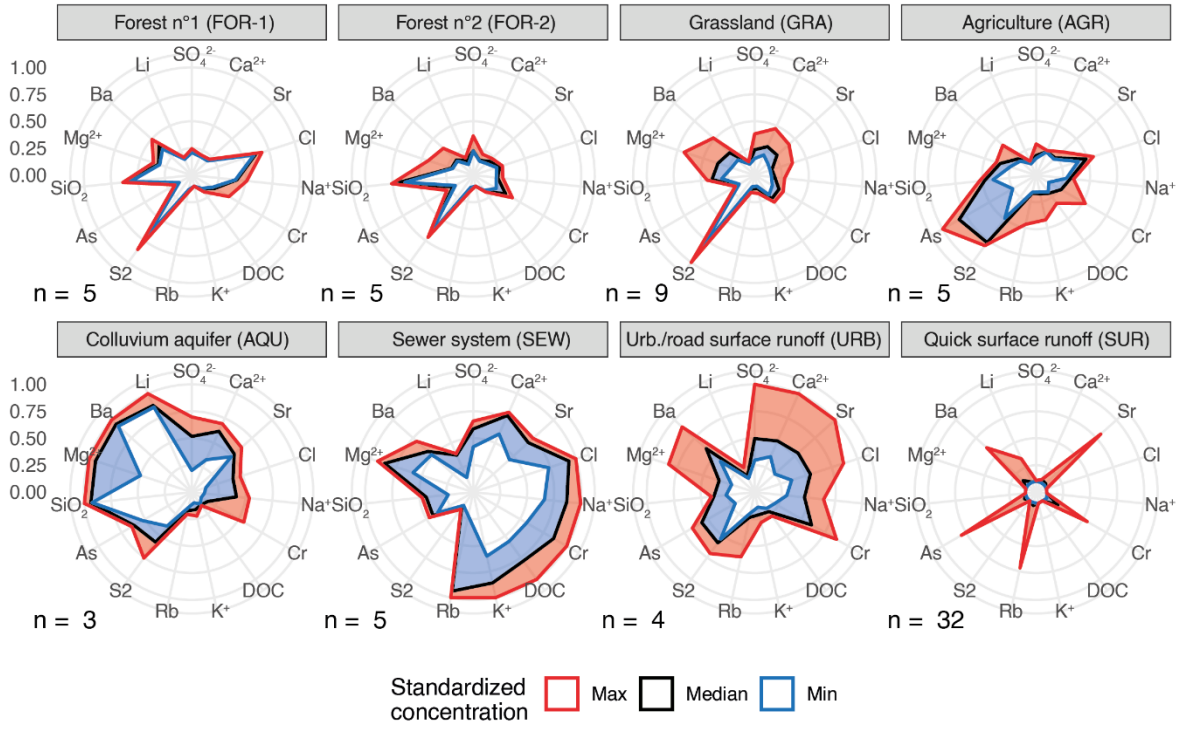

313

314 **Figure 5 – Biogeochemical signatures of the identified sources, in the form of a radar plot. The 15 tracers correspond to the optimal**
315 **selection resulting from the reductionist approach. Maximum, median and minimum concentrations are presented after**
316 **standardization across all 15 tracers. n: the number of samples per source; Urb: urban.**

317

https://doi.org/10.5194/egusphere-2025-2234
Preprint. Discussion started: 3 June 2025

The FOR-1 and FOR-2 signatures show low and stable concentrations, with high values of the parameter S2, which is a spectral slope calculated from absorption coefficients (350-400 nm), negatively correlated with the amount of aromatic carbon (Helms et al., 2008). The GRA signature is even more marked by high values of S2. Headwater from forests and grasslands is thus characterised by poorly aromatic DOM, which could be linked with high soil weathering (Wang et al., 2023). Boukra et al. (2023) showed similar results for surface waters from forest sub-catchments within the Ratier catchment, with a significant difference between water from forest watershed, less aromatic and water from agricultural areas (vineyards), more aromatic. Samples from the agricultural sub-catchment (AGR) also show higher values of the parameter S2, indicating low aromaticity, but are also characterised by even higher concentrations of the trace element As. According to Liu et al. (2020), significant concentrations of As can be observed in bovine manure, ranging from 2 to 17 mg/kg, which can explain the concentrations obtained for the AGR samples (median of 4.25 µg/L). The AQU signature is particularly characterised by high values of SiO_2, Mg^{2+}, Ba and Li. Grandjouan et al. (2023) pointed out that this runoff generating source is mainly fed by a colluvium aquifer, which significantly contributes to the Ratier stream volume outside of rainfall events, and attributed the high Li, Ba and Mg^{2+} concentrations to a geological origin. High SiO_2 concentrations are often observed in groundwater (Iorgulescu et al., 2005). The URB signature shows variable concentrations, with wide ranges, for SO_4^{2-}, Ca^{2+}, Sr, Cr, Mg^{2+} and Ba. This composition can be explained by the leaching of urban soils during rainy events, leading to the release of the elements that could have been emitted by urban and road pollutions sources and deposited at the surface of these soils. This phenomenon can be amplified by a first-flush effect, which favours the transport of elements for the first rains after long periods of dry weather (Deletic & Orr, 2005). The SEW signature is marked by high concentrations for Cl^-, Na^{2+}, Cr, DOC, K^+, Rb and Mg^{2+}, which is in line with the classical composition of wastewater seen in the literature (e.g. Eme & Boutin, 2015; Fröhlich et al., 2008). The variability observed for this source can be explained by the choice to collect the SEW samples during periods of rain (see Sect. 2.2.1). Therefore, water samples from the SEW source consist of a mix of wastewater, rainwater and road surface runoff, since this is a combined sewer network. Finally, the signature obtained for SUR shows very low concentrations for most of the 15 tracers, with the exception of high maximum concentrations for Sr, Cr, Rb, As, Ba. According to Becouze-Lareure (2010), these high concentrations are associated with atmospheric inputs to rainwater from the industrial Rhône valley, in the south-east of the Ratier catchment.

3.3 Hydrograph separation

3.3.1 Dry weather

Figure 6 shows the results of the mixing model decomposition for the 24 streamwater samples collected at the Mercier and Ratier outlets outside from rainfall events. Results for the Mercier catchment show little seasonality with similar results between low and high flow. The AGR source contributed the most at low flow (up to 40% of total runoff) and the GRA source at high flow (up to 50%). The SEW contribution was significant at both low and high flow conditions (between 10 and 50%), despite the absence of sewer overflow devices within the Mercier catchment. The higher contributions at low flow suggest a

https://doi.org/10.5194/egusphere-2025-2234
Preprint. Discussion started: 3 June 2025

continuous input of wastewater that may originate from the sewer system itself to the Mercier streamwater. Wastewater from domestic inputs or non-collective sanitation, not connected to the sewer system, could also contribute continuously to the Mercier streamwater.

Results for the Ratier catchment show a significant influence of the AQU source with a high seasonality. Contribution of AQU was predominant at low flow, up to 85% of total runoff. At high flow, groundwater from the colluvium aquifer was diluted by the other sources and GRA showed a major contribution (between 30 and 50%). The contributions estimated for SEW were lower than for the Mercier station (below 10%), supporting the hypothesis of a constant wastewater transfer to streamwater, as seen for the Mercier catchment, which may be diluted in the Ratier stream by the larger water flow.

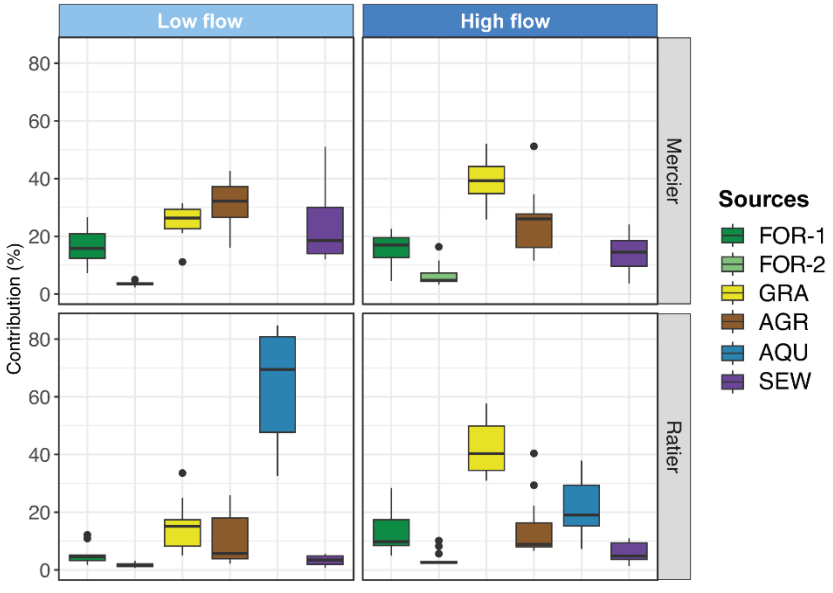

Figure 6 – Sources contribution to runoff estimated for dry weather samples by the application of a biogeochemical decomposition using a Bayesian approach for the Mercier and Ratier catchments. Boxplots represent the median contribution, interquartile range (1st and 3rd quartiles), minimum and maximum values. Low flow samples correspond to a mean daily discharge lower than 20 L/s and high flow samples to a mean daily discharge higher than 20 L/s.

3.3.2 Hydrological events: mean contributions

Figure 7 shows the mean of the source contributions estimated for each sampled hydrological event. These means were calculated from the individual results obtained by the application of the Bayesian mixing model approach on each streamwater sample (10 to 12 by event, see Sect. 2.2.2). Figure 7 also illustrates the uncertainty obtained for each event, in the form of the mean of the standard deviations obtained by applying each Bayesian mixing model decomposition, calculated from the sum of the squares of each deviation.

https://doi.org/10.5194/egusphere-2025-2234
Preprint. Discussion started: 3 June 2025

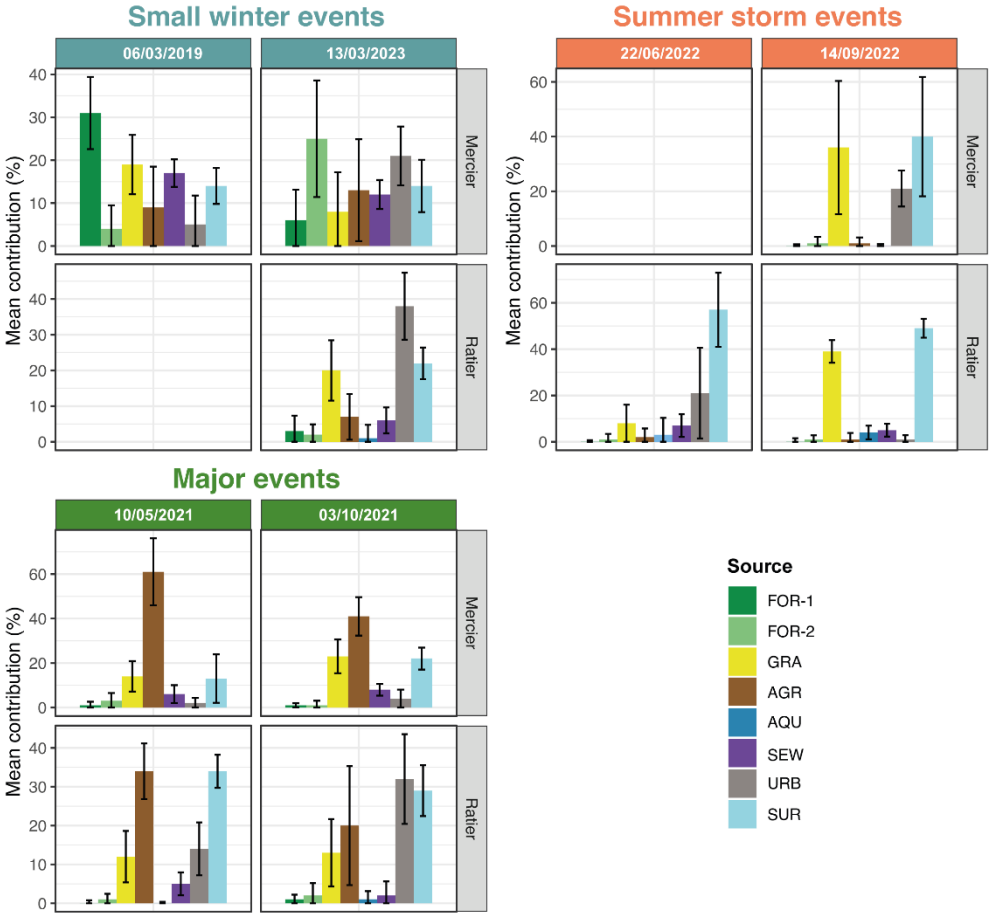

Figure 7 – Mean source contributions to the hydrological events sampled between March 2019 and March 2023 at the outlets of the Mercier and Ratier catchments. The contributions correspond to the mean of the results obtained for each samples decomposition by the Bayesian mixing model approach. The error bars correspond to the mean of the standard deviation calculated from the sum of the squares of the deviation. The events of 6 March 2019 at the Ratier station and 22 June 2022 at the Mercier station were not collected.

Results for small winter events show contrasted contributions. At the Mercier station, the major contribution was FOR-1 in March 2019 (31%) and FOR-2 in March 2023 (25%). In comparison, the contributions estimated at the Ratier station were much lower for both forest sources (5% in total), which is consistent with the results obtained in dry weather. Contributions of URB were significantly higher for the March 2023 event than for the March 2019 one, with 21% at the Mercier station and 38% at the Ratier station. This contrast can be explained by three times more rain in March 2023 (18 mm) than in March 2019 (7 mm). The source SEW showed high contributions at the Mercier station, similar to those estimated in dry weather (17 and 12% respectively for March 2023 and March 2019).

Results for the summer storm events showed predominant contributions of GRA, URB and SUR (>40%), but with relatively high uncertainties for the September 2022 event at the Mercier station compared to the Ratier station. The URB contribution

https://doi.org/10.5194/egusphere-2025-2234
Preprint. Discussion started: 3 June 2025

for the September 2022 event was lower at the Ratier (1%) than at the Mercier station (21%), which can be explained by the greater presence stormwater management structures for the Ratier than for the Mercier catchment. However, the contribution of URB was high for the June 2022 event at the Ratier station (21%). This result can be explained by the contribution from SEW (7%), which can be linked to sewer overflows. As these overflows are caused by excessive rainfall inputs in the sewer system, the volume transferred to streamwater during overflows is actually a mixture of wastewater, rainwater and urban surface water.

Results for both major events show predominant contributions for AGR: 61 and 41% at the Mercier station, 34 and 20% at the Ratier station. Uncertainty of the results were relatively low (<10%), with the exception of the October 2021 event at the Ratier station (up to 20%). The SUR and URB contributions were significant at the Ratier station (13 and 22% for URB, 34 and 29% for SUR). Those estimated at the Mercier station were lower, despite the high rainfall recorded for these events (92 and 89 mm). High SUR and URB contributions at the Ratier station can once again be explained by the sewer system overflows, spilling wastewater, rainwater and urban and road runoff water, which are less important in the Mercier catchment due to the absence of sewer overflow devices. The relative contributions estimated for SEW are low, but showed high wastewater volumes when related to the total flow volume observed for each event. By applying relative contributions to the observed discharge, we estimated SEW contributions in terms of volume at 900 and 2 000 m^3 at the Mercier and Ratier stations for the May 2021 event, and around 960 and 1 000 m^3 for the October 2021 event.

The hydro-meteorological conditions of the events appear to have a strong influence on the activated sources and their contributions. For the two small winter events, the contributions from grassland, agricultural areas, the sewer network and surface runoff are broadly consistent. However, there are significant differences in the contributions from urban and road runoff, which was higher in March 2023, and for those of the two forests between the March 2019 (FOR-1 as the main contribution) and the March 2023 events (FOR-2 as the main contribution). For summer storm events, the mean contributions estimated for both events are very consistent, with the exception of grassland and urban and road runoff. The major events showed the best consistency between the results for the Mercier and Ratier stations, despite some differences for sources linked to agriculture and urban road runoff. The spatial distribution of rainfall within the Ratier and Mercier catchments may also help explain the differences observed between the two stations. Local rainfall variability may have influenced the activation of specific sources, particularly those related to urban runoff and road surfaces.

The estimated results showed that similar sources have impacted the Mercier and Ratier catchments, with contributions showing similar trends. However, mean contributions showed significant differences, which will require a more precise study of the temporal variations over rain events.

3.3.3 Hydrological events: temporal variability of contributions

Figure 8 presents the results obtained by applying the biogeochemical mixing model to the Mercier and Ratier streamwater samples. It illustrates the temporal variability of the estimated contributions for each source. The results are presented in the form of bars whose sizes correspond to the instantaneous discharges associated to the decomposed samples.

https://doi.org/10.5194/egusphere-2025-2234
Preprint. Discussion started: 3 June 2025

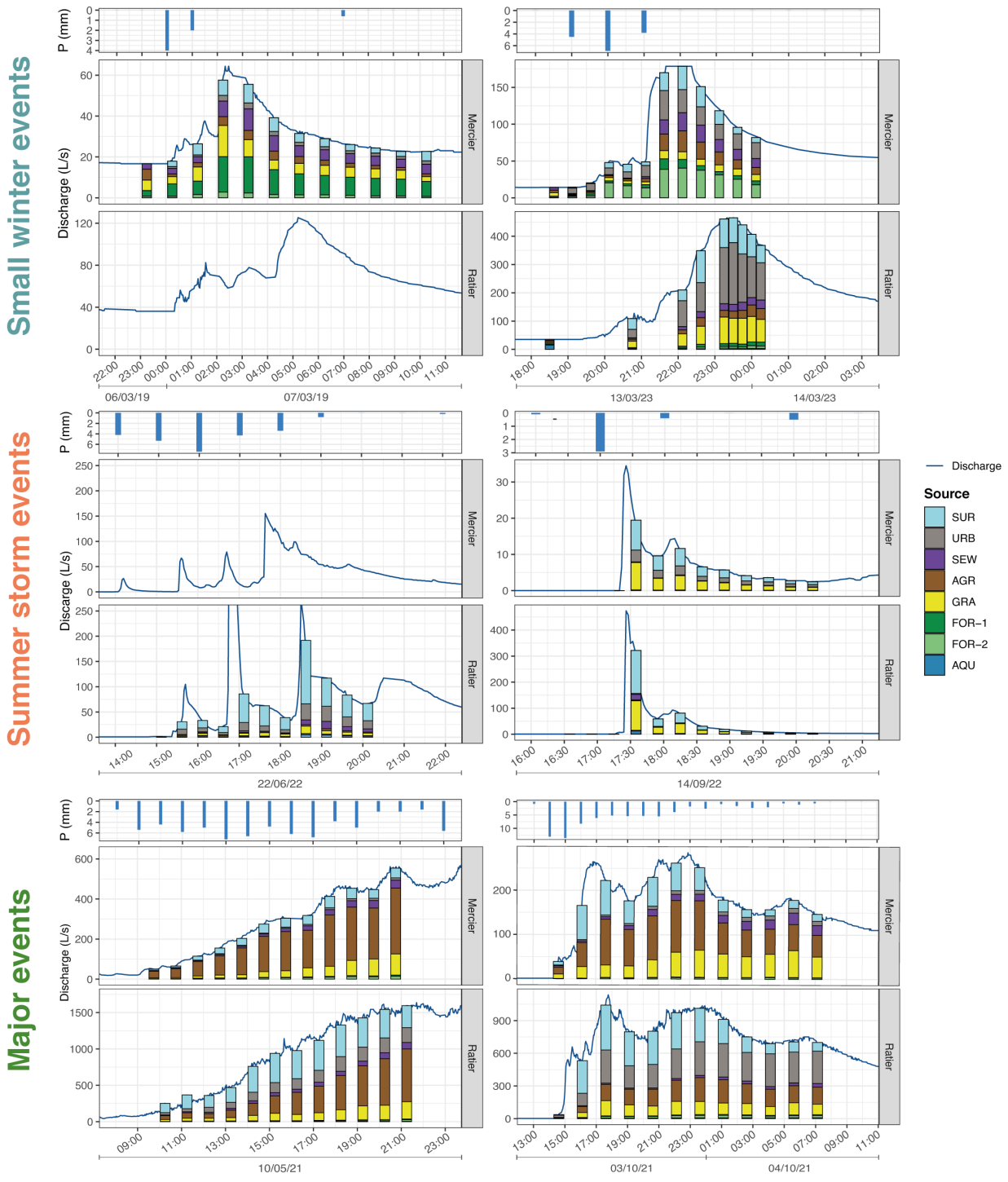

Figure 8 – Precipitation and hydrograph separation results for the sampled events at the Mercier and Ratier stations. The results are shown according to the total outlet discharge. The size of the bars corresponds to the instantaneous discharge associated to each sample.

https://doi.org/10.5194/egusphere-2025-2234
Preprint. Discussion started: 3 June 2025

In the case of the two small winter events of March 2019 and March 2023, the first sample was taken before the arrival of the rain. The contributions obtained for these samples prior to rainfall are consistent with the contributions estimated for samples collected under dry weather conditions: contribution of FOR-1 was around 15%, that of GRA around 30%, and that of AQU around 44%. As for dry weather results, the contribution of SEW was higher on the Mercier (up to 26%) than on the Ratier (13%). These results confirm the estimations obtained for dry weather. These contributions changed once the rain started, but remained stable until the end for each small winter event, despite the evolution of discharge. All these contributions estimated during rainfall are very close to the mean contributions shown in Figure 7. The contribution of urban and road surface runoff in March 2023 for the Ratier was the largest, right from the start of rainfall (52%), which might suggest particularly localized rainfall in urban areas. The contribution of the sewer system remained stable over the March 2019 event for the Mercier, showing a rising input of wastewater into the stream proportional to the total discharge. For the March 2023 event, the contribution of the sewer system decreased during rainfall, suggesting a dilution of wastewater by rainwater in the sewer system.

For the two summer storm events, most of the contributions remained relatively stable. The quick surface runoff contribution remained the largest and the most variable one. The estimated contributions for this source varied widely for the Ratier (from 20 to 65%), but were more stable for the Mercier (from 30 to 40%). The largest contributions were estimated during peak flows (65% for the Ratier for the June 2022 event and 50% for the September 2022 event). The estimated contributions from the sewer system also varied along the events for the Ratier: from 3 to 12% in June 2022 and from 2 to 14% in September 2022. As with quick surface runoff, the largest contribution of wastewater was estimated for the peak flow for the Ratier (7% of total discharge). Such high contribution might be linked to the overflow of the sewer system, via the sewer overflow device or any other points of the sewer system.

Finally, the contributions estimated for the two major events also showed low temporal variability. The predominant contribution was from agricultural areas, which varied from 40 to 60% for the Mercier, and from 20 to 30% for the Ratier. The contribution of quick surface runoff showed higher variability, particularly for the event of October 2021, with a predominant part during the peak flow (45% for the Mercier and 55% for the Ratier). For the May 2021 event, the quick surface runoff contribution never represented the majority, which can be explained by a less intense rainfall, favouring infiltration into the soil and the progressive rise of discharge. The contribution of wastewater was stable for the Ratier (around 5%), but increased significantly for the Mercier (up to 15%). These proportions represented contributions in volume up to 90 L/s at the Ratier for the May 2021 event, compared with the total discharge up to 1 500 L/s. In the case of this event, the cumulative contribution could therefore represent volumes of wastewater transferred to the stream between 1 000 and 2 000 m^3, equivalent to the mean daily wastewater discharge of 4 000 inhabitants (Aussel et al., 2004).

https://doi.org/10.5194/egusphere-2025-2234
Preprint. Discussion started: 3 June 2025

4 Discussion

4.1 Questioning the representativeness and nature of the sources

The application of a mixing model for decomposition of streamflow implies that the sources are well represented by their biogeochemical signatures. These signatures seem to have been particularly well defined for forests and grasslands. The signature of the colluvium aquifer was more variable, but remained significantly marked by high concentrations of Li, Ba and SiO_2 in all the samples. However, the signatures for other sources showed much more variability (Figure 5). The results question the representativeness of these signatures and the initial assumptions on which the identification and sampling of these sources were based.

Defining the biogeochemical signature of agricultural sources based on a single sub-catchment turned out to be challenging and highlighted three main difficulties. First, the catchment's characteristics made it difficult to delineate homogeneous sub-catchments associated with specific agricultural activities (e.g. crop culture, bovine breeding). Second, observing even a small flow at the outlets of agricultural sub-catchments was challenging due to the small size of these catchments and the predominance of crops and grasslands, which are linked with lower field capacity. As a result, only one agricultural sub-catchment could be identified and sampled. Third, the nature and intensity of agricultural activities can vary from one year to the next, and even within a single year, leading to seasonal variations in biogeochemical signatures. The use of more specific tracers, such as organic micropollutants, could improve the identification and characterization of agricultural sources, in a more precise manner than the general tracers used in this study, which were selected for their simplicity (Grandjouan et al., 2023). Previous studies have explored alternative approaches: El Azzi et al. (2016) compared commonly used pesticides concentrations with results from a chemical mixing model while Tran et al. (2019) investigated the presence of emerging contaminants, including veterinary products, to characterise different sources such as agricultural stormwater runoff, but also encountered high variability in concentrations.

For wastewater, our objective was to characterise the biogeochemical signature of the water discharged from the sewer system by overflow. To achieve this, we sampled water from the sewer system during rainfall events. Given that the water sampled is a mixture of wastewater and urban and road surface runoff, the obtained signature allowed us to estimate the contribution from the sewer system during these events. However, the results for dry weather conditions may be less reliable, as only wastewater is released through leaks in the sewer system. Ideally, the wastewater signature should have been built using samples collected from the sewer system under both dry weather and rainfall conditions. The mixing model therefore faces a first limitation as it is unable to distinguish wastewater alone from urban and road surface runoff. Kuhlemann et al. (2021) estimated the contribution of wastewater in the Erpe peri-urban catchment (Germany) using an end member mixing analysis, but also faced high uncertainties due to the similarities in concentrations between the composition of wastewater and other runoff sources. The use of isotopic tracers (e.g. δ^2H, $\delta^{18}O$) appears as a better way to estimate the contribution of wastewater in a Bayesian mixing model (Marx et al., 2021).

https://doi.org/10.5194/egusphere-2025-2234
Preprint. Discussion started: 3 June 2025

In the case of urban and road runoff (URB), the first flush effect, implying the leaching of urban soils which favours high concentrations of contaminants (e.g. Cu, Pb, Zn) after longer dry periods (Deletic & Orr, 2005), makes it difficult to characterise a proper and unique signature. Lin et al. (2024) used characteristics of DOM to estimate the contribution of road runoff in an urban catchment. They found that the water generated by road runoff exhibited high aromaticity of DOM. The values of the parameter S2, which is negatively correlated with aromaticity, were indeed lower for the URB signature than for the other sources. In their study, Fröhlich et al. (2008) deduced the urban surface runoff composition from the composition of streamwater during a peak flow, and from a Principal Component Analysis (PCA) as described in Christophersen & Hooper (1992). They used a PCA prior to the application of a mixing model, which allowed to confirm the correct number of sources and their biogeochemical composition.

Finally, as the quick surface runoff (SUR) composition was inferred from rainwater composition, it may be more or less distant from reality. The hypothesis of a quick surface runoff keeping the biogeochemical signature of rainwater is questionable as these waters can quickly accumulate elements (Langlois & Mehuys, 2003). Proper sampling of quick surface runoff should be done in order to better estimate their contributions to streamwater, although such sampling can be difficult. Yet, Fröhlich et al. (2008) showed in their study that the composition of stormflow headwaters was similar to precipitation, and characterised by low-mineralization. Their results suggest the predominant contribution of low-mineralized waters for several events, which support the use of the composition of rain to represent the quick surface runoff source.

4.2 Improvement of the hydrological perceptual model of the Ratier and Mercier catchments

An initial perceptual hydrological model of the Ratier catchment was built by Grandjouan et al. (2023). This model describes the general hydrological behaviour of the catchment and the main contributions to streamflow. The represented hydrological processes were deduced from catchment characteristics, field observations and a mixing model applied on the basis of the biogeochemical quality of streamwater at the Mercier and Ratier outlets at dry weather only. The extensive dataset obtained in the present study, including samples of runoff generating sources, and the contributions estimated in our study, allows for the improvement of this model, particularly in terms of hydrological behaviour at the hillslope scale.

Figure 9 illustrates the new hydrological perceptual model proposed for the Ratier and Mercier catchments. It represents the hydrological dynamics of each source inferred from the contributions estimated during dry weather and for different types of hydrological events. We considered small winter events to occur at high flow, summer storm event at low flow, and major events either at low or high flow.

https://doi.org/10.5194/egusphere-2025-2234
Preprint. Discussion started: 3 June 2025

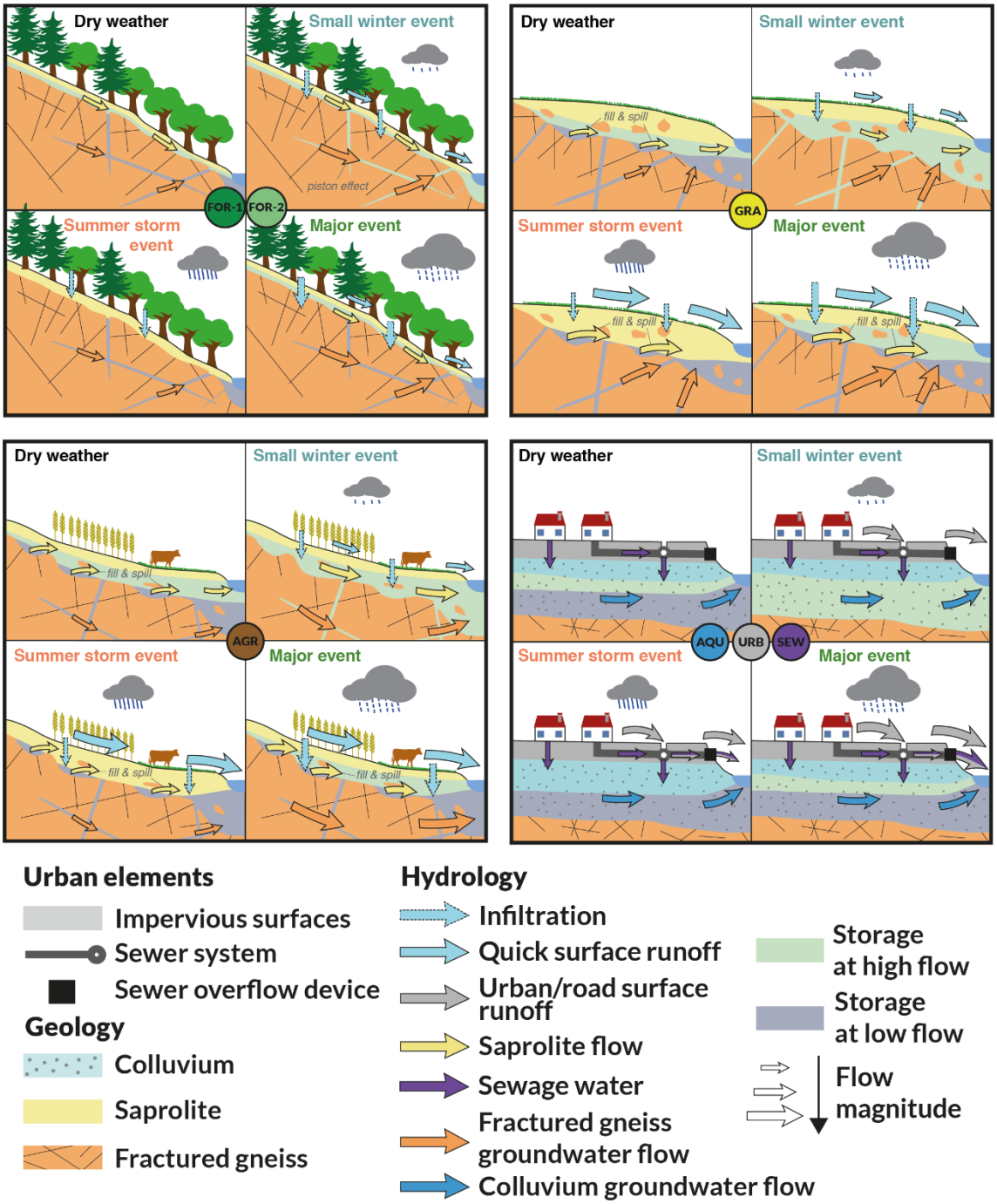

Figure 9 – Improved perceptual model of the Ratier catchment, initially build by Grandjouan et al. (2023). Main contributions, estimated by the mixing model, are illustrated according to the nature of the source and the four hydro-meteorological conditions studied, including dry weather, small winter event, summer storm event, major event. FOR : forest; GRA : grassland; AGR : agricultural; AQU : aquifer; URB : urban and road surface runoff; SEW : wastewater.

https://doi.org/10.5194/egusphere-2025-2234
Preprint. Discussion started: 3 June 2025

The two forest sources FOR-1 and FOR-2 were merged as they represent similar areas of the catchment. As their estimated contributions were close, we assumed they have a similar hydrological behaviour. These sources are characterised by a shallow or absent saprolite depth, with the fractured gneiss formation sometimes outcropping. The two forest sources were sampled for every campaign, independently from the hydro-meteorological conditions. As the saprolite horizon below the forest is unable to store a large volume of water, the constant flow generated by these springs is expected to originate mainly from fractures in the gneiss. These fractures are fed by infiltrating rainwater. Recharge water can have a piston effect, pushing the groundwater retained within the fractures towards the stream. Lachassagne et al. (2021) described a similar behaviour on another catchment characterised by fractured crystalline formations and thin saprolite layer (e.g. Alazard et al., 2016) with (1) a vertical piston effect in the saprolite layer and (2) a preferential deep horizontal flow in the fractures of the basement. This phenomenon could explain the major contribution of forests to the Mercier stream during small winter events. For summer storm event, the forest's contribution is minor, as the retention of rainwater by the vegetation is favoured over runoff (Bruijnzeel, 2004).

The runoff generated by grasslands could not be sampled under low flow conditions in dry weather. The highly variable thickness of the saprolite horizon in this part of the catchment - 1 to 20 m according to Goutaland (2009) – suggests the existence of throughs at the saprolite-gneiss interface in which water can be stored and released discontinuously. This process was described as "fill-and-spill" by Tromp-van Meerveld & McDonnell (2006), for the Panola catchment, characterised by a similar crystalline geological formation. During summer storm events, the quick surface runoff is favoured in grasslands. The water demand is lower than in forested or cultivated areas (Madani et al., 2017). Shi et al. (2021) showed that quick surface runoff is favoured with dry soils during summer periods.

Agricultural lands in the Ratier catchment are characterised by the same geological features as for grassland, and thus share similar hydrological behaviour. The main difference was observed for the summer storm event, where the contributions of agricultural lands were low compared to grasslands, which can be explained by the water demand of the crops culture. The high contributions during major events are difficult to interpret, and could be due to local discontinuities, or the leaching of agricultural soils containing agricultural-specific tracers. But it is difficult to assess on the genericity of the results for agricultural lands on the basis of a single sub-catchment.

The contribution of the urban impacted colluvium aquifer was constant, regardless of the hydro-meteorological conditions, as already shown by Grandjouan et al. (2023). The concentrations of human-specific fecal markers measured in several AQU samples suggest a contamination of the colluvium groundwater by wastewater. Grandjouan et al. (2023) showed the significant and constant input of wastewater into the soil and groundwater, through leaks in the sewer system or the use of septic tanks in residential areas disconnected from the public network. This input is particularly significant in the Mercier catchment, where wastewater represents a higher relative contribution than in the Ratier catchment when associated with their respective total flow. This wastewater contamination remains difficult to characterise in terms of both dynamics and volume. Numerical modelling of the sewer leakage appears to be a promising way of quantifying these impacts on groundwater (Nguyen et al., 2021).

https://doi.org/10.5194/egusphere-2025-2234
Preprint. Discussion started: 3 June 2025

5 Conclusions

The objective of this study was to identify runoff-generating sources in a small peri-urban catchment, and estimate their contribution to streamwater with a mixing model based on a biogeochemical dataset comprised of classical and original tracers. This approach highlighted eight main sources linked to the spatial characteristics of the catchment: two types of forest (FOR-1 and FOR-2), grassland (two sampled and merged as GRA), agricultural lands (AGR), a colluvium aquifer (AQU), wastewater from the sewer system (SEW), urban and road surface runoff (URB) and quick surface runoff (SUR). A comprehensive biogeochemical dataset was built to determine the signatures of these sources using a reductionist tracer selection approach. Each signature included 15 tracers: seven major parameters (Cl^-, SO_4^{2-}, Ca^{2+}, Na^{2+}, K^+, Mg^{2+}), six dissolved metals (As, Ba, Cr, Li, Rb, Sr) and two characteristics of DOM (DOC, spectral slope S2). Results showed that the use of indicators that are simple and cheap to analyse was sufficient to differentiate each source according to geological, pedological and land-use characteristics, or according to anthropogenic inputs.

The estimated source contributions were particularly stable in dry conditions, and significantly influenced by wastewater at the Mercier catchment, and by the colluvium groundwater at the Ratier catchment. At the hydrological event scale, the source contributions followed trends according to the hydro-meteorological state of the catchment: major contributions for forest, grassland and agricultural sources during small winter events, predominant quick surface runoff contributions for summer storm events, and major grassland and agricultural contributions for major events.

This approach showed the potential of the use of biogeochemical tracers to perform a spatial decomposition of water, based on the physical characteristics of a catchment, in addition to a more traditional vertical decomposition. This study also showed the need for precise methods to identify the runoff-generating sources and their biogeochemical signatures. An improvement of the approach would be a better characterisation of the most variable sources, such as agricultural lands, urban and road surface runoff and sewer system wastewater. Moreover, quick surface runoff needs to be collected and characterised to better estimate its contribution to streamwater. The initial campaign plan aimed to sample this runoff at various locations representing forest, grassland and agricultural areas. However, such sampling is challenging, as it requires being present at the right location and time due to the ephemeral nature of surface runoff. The deployment of automatic samplers could help overcome these limitations and improve data collection. Such sampling has already been implemented using a gutter-based collection system, as part of the ANR CHYPSTER project, in the Claduègne catchment (Ardèche, France).

This study demonstrated the effectiveness of the proposed method in estimating the water pathways and the main contributions within the studied catchments. The mixing model provided reliable estimates for several source contributions. Confidence in the results was reinforced by the use of additional tracers beyond those used in the mixing model, such as DOM characteristics, microbial parameters and other dissolved metals. The results obtained with the mixing model were consistent with the initial perceptual hydrological model built for the Ratier catchment, and allowed us to build an improved version at the hillslope scale. This new perceptual model provides a better understanding of the behaviour of these two nested catchments and their hydrological dynamics depending on each hydro-meteorological condition.

https://doi.org/10.5194/egusphere-2025-2234
Preprint. Discussion started: 3 June 2025

More broadly, the application of mixing models in relation to land use remains relatively unexplored in the literature. This study highlights the potential of such an approach when incorporating biogeochemical parameters and highlights the need for further research in this direction.

Appendices

Table A1 – Performance of analytical methods for dissolved organic carbon (DOC), total dissolved nitrogen (NTD), major ions and trace elements. Limits of quantification (LQ) and uncertainties (expanded U, k=2) were calculated according to standard method NF T90-210 (AFNOR, 2018) and NF ISO 11352 (AFNOR, 2013), respectively. For DOC, NTD and major ions, uncertainties were derived from results of interlaboratory tests. For trace elements, uncertainties were derived from regular analyses of Certified Reference Material TM-27-4 (lake water, Environment and Climate Change Canada).

	Parameter	Unit	LQ	Uncertainty
Organic matter	DOC	mgC/L	0,2	20%
	NTD	mgN/L	0,2	20%
Major ions	Ca^{2+}	mg/L	4,0	10%
	K^{+}	mg/L	1,0	15%
	Mg^{2+}	mg/L	1,0	13%
	Na^{+}	mg/L	1,0	12%
	NH_4^{+}	mg/L	0,02	14%
	Cl^{-}	mg/L	1,0	7%
	NO_2^{-}	mg/L	0,05	14%
	NO_3^{-}	mg/L	1,0	13%
	PO_4^{3-}	mg/L	0,1	14%
	SO_4^{2-}	mg/L	1,00	9%
	SiO_2	mgSi/L	0,5	12%
Trace elements	Al	µg/L	2,0	20%
	As	µg/L	0,010	20%
	B	µg/L	2,00	25%
	Ba	µg/L	0,01	10%
	Cd	µg/L	0,005	15%
	Co	µg/L	0,005	15%
	Cr	µg/L	0,02	20%
	Cu	µg/L	0,05	15%
	Fe	µg/L	0,10	15%
	Li	µg/L	0,010	20%
	Mn	µg/L	0,05	15%
	Mo	µg/L	0,010	20%
	Ni	µg/L	0,02	20%
	Pb	µg/L	0,01	20%
	Rb	µg/L	0,010	15%*
	Sr	µg/L	0,05	10%
	Ti	µg/L	0,05	25%
	U	µg/L	0,005	20%
	V	µg/L	0,005	20%
	Zn	µg/L	0,50	25%

* uncertainty calculated using coefficient of variation of measured values only (no certified value for this element)

https://doi.org/10.5194/egusphere-2025-2234
Preprint. Discussion started: 3 June 2025

Table A2 – Summary of analytical results for major parameters in source samples. Values are concentrations in mg/L. All analytical results, quantification results and quality controls are available at : https://entrepot.recherche.data.gouv.fr/dataverse/chypster/)

	BOU		VRY		VRN		REV		PNC	
Parameter	**Median**	**Range**	**Median**	**Range**	**Median**	**Range**	**Median**	**Range**	**Median**	**Range**
Ca^{2+}	11.1	10.5 - 12.3	6.2	5.5 – 13.0	22.7	21.1 - 40.4	14.6	12.1 - 18.6	15.7	15.3 - 16.9
Cl^-	51.0	49.5 - 56.9	16.0	13.2 - 18.6	6.63	5.8 - 26.7	9.7	7 - 16.7	38.0	30.7 - 44.8
K^+	1.0	1.0 – 1.0	1.0	1.0 – 1.0	1.6	1.5 - 2.6	1.0	1.0 – 1.0	2.7	2.2 - 8.3
Mg^{2+}	2.8	2.7 - 3.2	1.9	1.8 - 3.7	3.2	3.0 - 5.7	2.4	2.0 - 3.1	3.0	2.2 - 3.3
Na^+	26.8	25.7 - 34.2	11.3	10.2 - 15.3	8.6	8.10 - 15.4	6.3	5.6 - 7.8	18.6	15.6 - 21.1
NH_4^+	0.02	0.02 - 0.02	0.02	0.02 - 0.03	0.02	0.02 - 0.05	0.02	0.02 - 0.08	0.06	0.02 - 2.09
NO_2^-	0.05	0.05 - 0.05	0.05	0.05 - 0.05	0.05	0.05 - 0.05	0.05	0.05 - 0.05	0.05	0.05 - 0.19
NO_3^-	5.60	2.50 - 18.3	3.80	1.40 - 16.8	11.1	7.00 - 24.9	1.79	1.00 - 11.4	2.00	1.00 - 13.4
DTN	1.40	0.75 - 4.25	1.10	0.50 - 3.80	2.40	1.85 - 5.20	0.83	0.65 - 2.65	0.85	0.65 - 4.30
PO_4^{3-}	0.10	0.10 - 0.10	0.10	0.10 - 0.10	0.10	0.10 - 0.10	0.10	0.10 - 0.10	0.10	0.10 - 0.10
SiO_2	20.4	18.4 - 21.1	24.1	20.8 - 25.6	12.7	10.7 - 13.5	11.1	8.3 - 11.9	14.9	11.9 - 16.8
SO_4^{2-}	13.8	12.2 - 15.9	14.1	13.6 – 28.0	18.7	14.9 – 30.0	9.3	6.6 - 13.4	9.5	6.8 - 20.4

	COR		PLR		RES	
Parameter	**Median**	**Range**	**Median**	**Range**	**Median**	**Range**
Ca^{2+}	55.8	25.3 - 64	45.4	28.6 - 96.3	72.8	52.9 - 76.2
Cl^-	29.9	4.6 - 45.7	43.4	25.9 - 74.4	80.8	61.9 - 87.4
K^+	2.9	0.9 - 3.8	3.5	1.9 - 5.2	18.3	12.5 - 21.5
Mg^{2+}	7.5	4.2 - 8.2	3.0	2.0 - 6.9	7.1	4.9 - 7.6
Na^+	26.5	2.3 – 37.0	30.3	17.0 - 44.7	63.2	46.4 - 73.6
NH_4^+	0.07	0.03 - 0.33	0.04	0.02 - 0.20	48.6	32.4 - 78.7
NO_2^-	0.17	0.05 - 0.51	0.22	0.05 - 0.37	0.81	0.05 - 1.03
NO_3^-	12.7	5.40 - 17.7	14.9	8.82 - 38.4	5.56	1.00 - 12.4
DTN	3.55	2.25 - 4.30	3.80	2.00 - 8.15	43.6	30.4 – 67.0
PO_4^{3-}	0.26	0.23 - 0.35	0.32	0.11 - 0.37	9.81	7.50 - 12.9
SiO_2	32.0	15.5 - 34.8	11.1	6.8 – 12.0	13.3	5.5 - 14.8
SO_4^{2-}	43.7	11.4 - 62.2	41.6	21.1 - 93.2	50.8	33.8 - 58.3

https://doi.org/10.5194/egusphere-2025-2234
Preprint. Discussion started: 3 June 2025

Table A3 – Summary of analytical results for dissolved metals in source samples. Values are concentrations in µg/L. All analytical results, quantification results and quality controls are available at: https://entrepot.recherche.data.gouv.fr/dataverse/chypster/)

	BOU		VRY		VRN		REV		PNC	
Parameter	Median	Range	Median	Range	Median	Range	Median	Range	Median	Range
Al	126	82.8 - 142	62.5	45.3 - 105	43.2	8.40 - 70.5	75.1	24.3 - 102	29.2	18.9 - 55.9
As	0.49	0.25 - 0.52	0.73	0.58 - 1.11	0.63	0.43 - 0.68	0.53	0.45 - 0.66	4.25	0.93 - 5.28
B	3.00	2.80 - 4.70	3.90	3.70 - 5.00	11.4	8.30 - 18.6	2.80	2.20 - 4.20	2.60	0.20 - 7.30
Ba	20.0	17.9 - 24.4	10.4	9.70 - 18.4	15.4	13.3 - 25.4	13.4	10.4 - 18.7	11.2	9.73 - 20.5
Cd	0.073	0.064 - 0.096	0.023	0.010 - 0.030	0.008	0.005 - 0.021	0.020	0.012 - 0.027	0.009	0.005 - 0.024
Co	0.160	0.144 - 0.173	0.109	0.063 - 0.320	0.125	0.112 - 0.135	0.139	0.115 - 0.213	0.779	0.079 - 1.28
Cr	0.23	0.20 - 0.43	0.37	0.23 - 0.46	0.19	0.15 - 0.29	0.30	0.24 - 0.31	0.26	0.08 - 0.61
Cu	0.42	0.10 - 0.67	0.66	0.10 - 2.75	3.70	3.23 - 4.23	1.77	0.77 - 2.89	0.94	0.74 - 11.3
Fe	24.4	9.10 - 34.1	46.6	13.1 - 106	30.3	5.79 - 59.6	35.3	16.9 - 48.8	285	13.4 - 897
Li	1.84	1.75 - 2.27	1.42	0.29 - 2.15	0.692	0.622 - 0.753	0.756	0.391 - 1.08	0.759	0.483 - 1.23
Mn	11.7	9.15 - 12.2	12.6	4.84 - 34.6	1.17	0.66 - 4.03	3.86	1.16 - 8.52	556	1.17 - 1209
Mo	0.045	0.029 - 0.058	0.048	0.029 - 0.057	0.158	0.108 - 0.185	0.0305	0.010 - 0.037	0.304	0.067 - 0.488
Ni	1.13	1.09 - 1.66	1.42	1.14 - 1.67	1.35	0.99 - 2.80	0.99	0.85 - 1.61	0.88	0.44 - 1.08
Pb	0.019	0.005 - 0.032	0.130	0.082 - 0.146	0.013	0.005 - 0.094	0.014	0.005 - 0.024	0.060	0.005 - 0.312
Rb	0.850	0.719 - 1.21	0.724	0.327 - 1.06	0.716	0.598 - 1.19	0.396	0.209 - 0.471	1.30	1.13 - 6.53
Sr	44.1	41.4 - 51.3	40.5	26.5 – 56.0	81.4	75.5 - 138	46.8	27.0 - 68.2	58.9	51.7 - 94.4
Ti	0.52	0.05 - 1.29	1.26	0.27 - 3.94	0.90	0.18 - 2.14	1.80	0.58 - 2.68	0.86	0.75 - 2.73
U	0.298	0.211 - 0.349	0.157	0.005 - 0.303	0.244	0.117 - 0.316	0.148	0.033 - 0.257	0.120	0.079 – 1.00
V	0.289	0.213 - 0.357	0.331	0.229 - 0.403	0.308	0.276 - 0.344	0.297	0.276 - 0.683	0.381	0.258 - 1.02
Zn	1.74	1.33 - 2.16	1.57	0.10 - 1.85	2.63	1.79 - 6.81	2.18	0.93 - 2.76	1.95	1.30 - 73.4

	COR		PLR		RES	
Parameter	Median	Range	Median	Range	Median	Range
Al	13.8	7.99 - 97.9	54.3	15.5 - 62.7	17.1	13.9 - 47.5
As	3.05	1.99 - 3.47	2.75	0.68 - 3.34	1.97	1.68 - 2.20
B	17.7	14.9 - 46.5	31.4	15.6 - 36.4	47.9	21.3 - 89.6
Ba	46.4	28.8 - 49.2	29.7	21.0 - 44.5	27.8	25.6 - 34.7
Cd	0.008	0.005 - 0.013	0.027	0.014 - 0.058	0.021	0.014 - 0.107
Co	0.116	0.066 - 0.137	0.276	0.145 - 0.482	0.503	0.122 - 0.579
Cr	0.226	0.033 - 0.65	0.72	0.19 - 1.08	1.06	0.67 - 1.25
Cu	2	0.1 - 3.66	8.57	1.07 - 14.3	19.6	9.98 - 24.8
Fe	64.1	37.1 - 99.5	22.8	8.00 - 62.3	50.4	27.9 - 104
Li	21.1	9.93 - 24.9	1.79	1.15 - 4.22	7.68	1.40 - 8.08
Mn	33.2	17.8 - 81.6	13.8	0.69 - 59.7	28.9	3.91 - 54.4
Mo	0.901	0.747 - 1.19	1.2	0.05 - 1.57	1.06	0.749 - 1.39
Ni	0.509	0.02 - 0.594	0.96	0.58 - 1.19	1.56	0.56 - 2.15
Pb	0.124	0.049 - 0.202	0.142	0.039 - 0.588	0.460	0.322 - 0.528
Rb	1.55	0.831 - 2	2.53	1.81 - 9.15	14.9	2.22 – 16.0
Sr	181	126 - 219	186	64.1 - 379	247	148 - 272
Ti	0.236	0.126 - 5.67	0.48	0.32 - 3.07	1.45	0.52 - 2.13
U	0.558	0.544 - 0.906	1.69	0.100 - 2.80	1.29	1.12 - 2.73
V	0.919	0.561 - 0.985	1.51	0.408 - 3.53	0.598	0.272 - 1.30
Zn	13.6	4.3 - 13.7	18.6	4.56 - 48.6	36.6	20.4 - 44.2

https://doi.org/10.5194/egusphere-2025-2234
Preprint. Discussion started: 3 June 2025

Table A4 – Summary of analytical results for characteristics of dissolved organic matter in source samples. All analytical results, quantification results and quality controls are available at : https://entrepot.recherche.data.gouv.fr/dataverse/chypster/)

		BOU		VRY		VRN		REV		PNC	
Parameter	**Unit**	**Median**	**Range**	**Median**	**Range**	**Median**	**Range**	**Median**	**Range**	**Median**	**Range**
DOC	mg/L	2.9	2.7 - 4.6	4.2	3.8 - 4.7	7.5	6.2 - 8.2	8.4	8.4 - 10.1	5.3	4.6 - 10.8
E2:E3	-	7.4	6.8 - 7.7	6.4	6.1 - 6.6	6.7	6.3 - 6.9	6.9	6.4 - 7.3	4.7	4.5 - 6.3
E2:E 4	-	24.9	21.2 - 28.9	20.6	19.2 - 21.8	25.2	22.8 - 26.5	27.7	24.0 - 29.6	17.7	13.5 - 21.5
E3:E4	-	6.9	6.2 - 7.1	5.9	5.7 - 6.1	6.7	6.3 - 7.0	7.1	6.5 - 7.6	5.3	4.5 - 6.4
E4:E6	-	8.8	3.5 - 12.8	10.2	7.2 - 17.4	11.2	6.4 - 30.3	9.1	6.0 - 12.4	11.6	5.9 - 21.1
SUVA	L/mgC/m	2.2	2.1 - 2.4	2.7	2.5 - 3.0	2.9	2.6 - 3.0	2.8	2.6 - 3.0	3.1	2.9 - 4.3
S1	nm-1	0.0160	0.0158 - 0.0163	0.0156	0.0153 - 0.0158	0.0153	0.0151 - 0.0155	0.0151	0.0150 - 0.0155	0.0134	0.0119 - 0.0144
S2	nm-1	0.0196	0.0184 - 0.0203	0.0185	0.0183 - 0.0187	0.0205	0.0199 - 0.0209	0.0213	0.0207 - 0.0220	0.0194	0.0162 - 0.0198
SR	-	0.83	0.79 - 0.86	0.84	0.83 - 0.86	0.76	0.72 - 0.77	0.71	0.70 - 0.73	0.71	0.60 - 0.83
Mn-254	Da	417	323 - 460	542	394 - 593	616	548 - 695	607	596 - 636	569	526 - 703
Mw-254	Da	1718	1352 - 2365	1644	1049 - 2364	1543	1146 - 1766	1266	1188 - 1649	1423	1198 - 1858
disp-254	-	4.19	3.02 - 7.04	2.77	2.52 - 5.13	2.42	1.86 - 2.96	2.05	1.93 - 2.77	2.31	2.02 - 3.28
A0-254	-	4552	2486 - 7349	4772	2165 - 8337	4627	407 - 10478	2404	1501 - 7710	2265	1209 - 4962
A1-254	-	21850	15215 - 34702	47737	46348 - 59736	117263	86123 - 138631	110027	104294 - 117502	67331	50782 - 114518
A2-254	-	48675	38354 - 83965	78227	70245 - 93519	188721	146038 - 204308	216676.5	185118 - 228952	121649	80952 - 176082
A3-254	-	54560	47984 - 128755	65957	54730 - 85950	96041	77790 - 123959	112563	102393 - 121161	62096	53834 - 112852

		COR		PLR		RES	
Parameter	**Unit**	Median	Range	Median	Range	Median	Range
DOC	mg/L	3.5	2.0 - 10.1	6.1	4.4 - 8.4	32.7	22.1 - 42.6
E2:E3	-	5.2	4.8 - 6.9	5.9	5.8 - 6.1	5.4	4.9 - 7.6
E2:E4	-	14.9	11.9 - 23.3	18.9	17.2 - 20.6	11.3	10.5 - 14.9
E3:E4	-	5.0	4.6 - 7.1	5.5	5.3 - 5.9	4.3	3.9 - 5.7
E4:E6	-	5.6	3.0 - 15.1	9.1	7.8 - 10.5	6.8	5.9 - 8.7
SUVA	L/mgC/m	2.0	0.8 - 2.6	2.8	2.4 - 3.0	1.3	0.9 - 1.4
S1	nm-1	0.0123	0.0118 - 0.0145	0.0144	0.0144 - 0.0153	0.0161	0.0104 - 0.0168
S2	nm-1	0.0163	0.0150 - 0.0192	0.0172	0.0167 - 0.0186	0.0127	0.0123 - 0.0128
SR	-	0.80	0.64 - 0.85	0.84	0.77 - 0.92	1.28	0.82 - 1.33
Mn-254	Da	451	434 - 670	727	621 - 885	424	383 - 579
Mw-254	Da	2031	941 - 2432	1765	1571 - 1974	1390	1204 - 2201
disp-254	-	3.03	2.17 - 5.39	2.21	2.00 - 3.18	3.14	2.88 - 4.00
A0-254	-	4797	144 - 7402	3085	2560 - 9811	6713	4296 - 14343
A1-254	-	33782	18214 - 53643	128469	65410 - 156480	73927	61653 - 100544
A2-254	-	45994	20069 - 65362	137524	86234 - 207418	116338	93322 - 171777
A3-254	-	43102	16900 - 55750	54241	35715 - 114897	129258	85384 - 218065

https://doi.org/10.5194/egusphere-2025-2234
Preprint. Discussion started: 3 June 2025

Table A5 – Summary of analytical results for microbial parameters in source samples. Values are concentrations in log10 number of copies/100 mL. All analytical results, quantification results and quality controls are available at : https://entrepot.recherche.data.gouv.fr/dataverse/chypster/)

	BOU		VRY		VRN		REV		PNC	
Parameter	**Median**	**Range**	**Median**	**Range**	**Median**	**Range**	**Median**	**Range**	**Median**	**Range**
G16S	7.3	7.0 - 7.5	7.8	7.4 - 9.1	7.8	7.8 - 8.6	8.8	8.8 - 8.9	8.4	7.2 - 9.4
BTT	3.7	2.6 - 4.2	4.0	0.0 - 5.1	5.0	0.0 - 5.5	6.3	0.0 - 6.7	6.2	5.1 - 6.7
HF183	0.0	0.0 – 0.0	0.0	0.0 – 0.0	0.0	0.0 - 1.9	0.0	0.0 – 0.0	0.0	0.0 – 0.0
rum-2-bac	0.0	0.0 – 0.0	0.0	0.0 – 0.0	0.0	0.0 – 0.0	0.0	0.0 – 0.0	0.0	0.0 – 6.0
BTS	0.0	0.0 - 3.5	0.0	0.0 – 0.0	0.0	0.0 - 2.2	0.0	0.0 – 0.0	0.0	0.0 – 3.0
int1	0.0	0.0 - 4.1	0.0	0.0 - 3.9	0.0	0.0 - 4.8	3.3	0.0 - 3.4	0.0	0.0 – 0.0
.int2	0.0	0.0 - 3.8	0.0	0.0 – 0.0	0.0	0.0 – 0.0	0.0	0.0 – 0.0	1.4	0.0 - 3.4

	COR		PLR		RES	
Parameter	**Median**	**Range**	**Median**	**Range**	**Median**	**Range**
G16S	9.4	8.6 - 9.6	9.4	9.2 - 9.5	10.4	9.5 - 11.4
BTT	6.3	6.2 - 7.3	6.5	6.5 - 6.6	8.80	7.9 - 9.6
HF183	3.7	3.5 - 6.3	3.5	3.1 - 3.6	7.05	5.7 - 7.5
rum-2-bac	0.0	0.0 – 0.0	0.0	0.0 – 0.0	4.15	3.4 - 4.6
BTS	3.6	3.3 - 4.6	5.1	5.0 - 6.2	7.05	6.6 - 7.9
int1	0.0	0.0- 3.0	4.0	0.0 - 4.5	5.25	4.3 – 6.0
int2	4.4	0.0 – 6.0	2.8	0.0 - 3.4	6.30	5.0- 6.5

https://doi.org/10.5194/egusphere-2025-2234
Preprint. Discussion started: 3 June 2025

Data availability

Hydro-meteorological data and biogeochemical data at the catchment outlets during dry weather is available online at https://bdoh.irstea.fr/YZERON/station/V3015810 and https://bdoh.irstea.fr/YZERON/station/V301502401, respectively for the Mercier and the Ratier station (https://doi.org/10.57745/VVQ2X9; https://doi.org/10.17180/obs.yzeron). Metadata relative to the sampling of sources and of the catchment outlets are detailed at: https://doi.org/10.57745/K3S9YV. Biogeochemical data of the sources and at the catchment outlets during hydrological events is available at https://doi.org/10.57745/HQPIFQ for major parameters and dissolved metals, and at https://doi.org/10.57745/IYJ2VE for characteristics of DOM.

Author contributions

Olivier Grandjouan: Writing – original draft, Visualization, Methodology, Investigation, Formal analysis, Conceptualization. **Flora Branger**: Writing – review & editing, Investigation, Methodology, Conceptualization. **Matthieu Masson**: Writing – review & editing, Investigation, Methodology, Conceptualization. **Benoit Cournoyer**: Writing – review & editing, Investigation, Methodology. **Nicolas Robinet**: Writing – review & editing, Investigation, Methodology. **Pauline Dusseux**: Writing – review & editing, Investigation, Methodology. **A. Dominguez Lage**: Writing – review & editing, Investigation, Methodology. **Marina Coquery**: Writing – review & editing, Investigation, Methodology, Conceptualization, Funding acquisition, Project administration

Declaration of competing interest

The authors declare that they have no known competing financial interests or personal relationships that could have appeared to influence the work reported in this paper.

Acknowledgements

Authors thanks Corinne Brosse-Quilgars, Lysiane Dherret, Loïc Richard, Aymeric Dabrin, Amandine Daval and Christelle Margoum of the Aquatic Chemistry Laboratory team of RiverLy (INRAE), and Laurence Marjolet and B. Youenou of UMR Ecologie Microbienne (VetAgro Sup) for the analysis of the samples, as well as M. Lagouy (INRAE, RiverLy) for field sampling. We also thank the OTHU (Field Observatory in Urban Hydrology) and OZCAR (Critical Zone Observatories: Research and Application) observatories for data provision. This work was carried out in the frame of a PhD, which was partly funded by EUR H2O Lyon, and in the frame of the CHYPSTER research project partly funded by the French National Research

https://doi.org/10.5194/egusphere-2025-2234
Preprint. Discussion started: 3 June 2025

Agency (ANR-21-CE34-0013-01) and the IDESOC project granted by the ZABR – Rhone Basin LTSER within the Water Agency RMC – RB LTSER funding agreement.

References

AFNOR. (2013). Standard method NF ISO 11352. Water Quality—Estimation of measurement uncertainty based on validation and quality control data.

AFNOR. (2018). Standard method NF T90-210. Water quality—Protocol for the intial method performance assesment in a laboratory.

Alazard, M., Boisson, A., Maréchal, J.-C., Perrin, J., Dewandel, B., Schwarz, T., Pettenati, M., Picot-Colbeaux, G., Kloppmann, W., & Ahmed, S. (2016). Investigation of recharge dynamics and flow paths in a fractured crystalline aquifer in semi-arid India using borehole logs : Implications for managed aquifer recharge. Hydrogeology Journal, 24(1), 35. https://doi.org/10.1007/s10040-015-1323-5

Aussel, H., Bâcle, C. L., & Dornier, G. (2004). Le traitement des eaux usées. INRS.

Baduel, M. (2022). Etablissement d'un modèle de mélange d'eau permettant de calculer la contribution de sous-bassins homogène à l'exutoire [Master]. Mémoire de Master, Université Paris-Est Créteil.

Barthold, F. K., Wu, J., Vaché, K. B., Schneider, K., Frede, H.-G., & Breuer, L. (2010). Identification of geographic runoff sources in a data sparse region : Hydrological processes and the limitations of tracer-based approaches. Hydrological Processes, 24(16), 2313-2327. https://doi.org/10.1002/hyp.7678

Becouze-Lareure, C. (2010). Caractérisation et estimation des flux de substances prioritaires dans les rejets urbains par temps de pluie sur deux bassins versants expérimentaux (p. 1 vol. (298 p.)) [Phd, Thèse de doctorat]. http://www.theses.fr/2010ISAL0089

Begum, M. S., Park, H.-Y., Shin, H.-S., Lee, B.-J., & Hur, J. (2023). Separately tracking the sources of hydrophobic and hydrophilic dissolved organic matter during a storm event in an agricultural watershed. Science of The Total Environment, 873, 162347. https://doi.org/10.1016/j.scitotenv.2023.162347

Benjamin, M. M. (2014). Water Chemistry : Second Edition. Waveland Press. https://books.google.fr/books?id=dr-VBAAAQBAJ

Bétemps, M. (2021). Diagnostic de l'occupation du sol et de l'utilisation des produits chimiques sur le bassin versant de l'Yzeron (Rhône) : Utilisation combinée d'enquêtes et de données cartographiques pour identifier les sources de contaminants et leur localisation. [Master]. Mémoire de Master, Université Grenobles Alpes, Laboratoire IGE Cermosem.

Beven, K. (2012). Rainfall-runoff modelling : The primer, second edition (Vol. 457). John Wiley & Sons, Ltd.

Birkel, C., & Soulsby, C. (2015). Advancing tracer-aided rainfall-runoff modelling : A review of progress, problems and unrealised potential. Hydrological Processes, 29(25), 5227-5240. https://doi.org/10.1002/hyp.10594

Birkinshaw, S. J., O'Donnell, G., Glenis, V., & Kilsby, C. (2021). Improved hydrological modelling of urban catchments using runoff coefficients. Journal of Hydrology, 594, 125884. https://doi.org/10.1016/j.jhydrol.2020.125884

Bomboï, M. T., & Hernandez, A. (1991). Hydrocarbons in urban runoff : Their contribution to thewastewaters. Water Research, 25(5), 557-565.

Bouchali, R., Mandon, C., Danty - Berger, E., Géloën, A., Marjolet, L., Youenou, B., Pozzi, A. C. M., Vareilles, S., Galia, W., Kouyi, G. L., Toussaint, J.-Y., & Cournoyer, B. (2024). Runoff microbiome quality assessment of a city center rainwater harvesting zone shows a differentiation of pathogen loads according to human mobility patterns. International Journal of Hygiene and Environmental Health, 260, 114391. https://doi.org/10.1016/j.ijheh.2024.114391

Boukra, A., Masson, M., Brosse, C., Sourzac, M., Parlanti, E., & Miège, C. (2023). Sampling terrigenous diffuse sources in watercourse : Influence of land use and hydrological conditions on dissolved organic matter characteristics. Science of The Total Environment, 872, 162104. https://doi.org/10.1016/j.scitotenv.2023.162104

https://doi.org/10.5194/egusphere-2025-2234
Preprint. Discussion started: 3 June 2025

Branger, F., Kermadi, S., Jacqueminet, C., Michel, K., Labbas, M., Krause, P., Kralisch, S., & Braud, I. (2013). Assessment of the influence of land use data on the water balance components of a peri-urban catchment using a distributed modelling approach. Journal of Hydrology, 505, 312-325. https://doi.org/10.1016/j.jhydrol.2013.09.055

Braud, I., Branger, F., Chancibault, K., Jacqueminet, C., Breil, P., Chocat, B., Debionne, S., Dodane, C., Honegger, A., Joliveau, T., Kermadi, S., Leblois, E., Lipeme Kouyi, G., Michel, K., Mosini, M. L., Renard, F., Rodriguez, F., Sarrazin, B., Schmitt, L., … Viallet, P. (2011). Assessing the vulnerability of PeriUrban rivers. Rapport scientifique final du projet AVuPUR (ANR-07-VULN-01) (p. 96) [Research Report]. IRSTEA. https://hal.inrae.fr/hal-02596619

Bruijnzeel, L. A. (2004). Hydrological functions of tropical forests : Not seeing the soil for the trees? Agriculture, Ecosystems & Environment, 104(1), 185-228. https://doi.org/10.1016/j.agee.2004.01.015

Burns, D. A., McDonnell, J., Hooper, R. P., Peters, N. E., Freer, J. E., Kendall, C., & Beven, K. (2001). Quantifying contributions to storm runoff through end-member mixing analysis and hydrologic measurements at the Panola Mountain research watershed (Georgia, USA). Hydrological Processes, 15(10), 1903-1924. https://doi.org/10.1002/hyp.246

Cabral Nascimento, R., Jamil Maia, A., Jacques Agra Bezerra da Silva, Y., Farias Amorim, F., Williams Araújo do Nascimento, C., Tiecher, T., Evrard, O., Collins, A. L., Miranda Biondi, C., & Jacques Agra Bezerra da Silva, Y. (2023). Sediment source apportionment using geochemical composite signatures in a large and polluted river system with a semiarid-coastal interface, Brazil. CATENA, 220, 106710. https://doi.org/10.1016/j.catena.2022.106710

Charters, F. J., Cochrane, T. A., & O'Sullivan, A. D. (2016). Untreated runoff quality from roof and road surfaces in a low intensity rainfall climate. Science of The Total Environment, 550, 265-272. https://doi.org/10.1016/j.scitotenv.2016.01.093

Chocat, B., Krebs, P., Marsalek, J., Rauch, W., & Schilling, W. (2001). Urban drainage redefined : From stormwater removal to integrated management. Water Science and Technology, 43(5), 61-68. https://doi.org/10.2166/wst.2001.0251

Christophersen, N., & Hooper, R. P. (1992). Multivariate analysis of stream water chemical data : The use of principal components analysis for the end-member mixing problem. Water Resources Research, 28(1), 99-107. https://doi.org/10.1029/91WR02518

Christophersen, N., Neal, C., Hooper, R., Vogt, R., & Andersen, S. (1990). Modeling streamwater chemistry as a mixture of soil water end-members—A step towards second generation acidification models. Journal of Hydrology, 116, 307-320. https://doi.org/10.1016/0022-1694(90)90130-P

Colin, Y., Bouchali, R., Marjolet, L., Marti, R., Vautrin, F., Voisin, J., Bourgeois, E., Rodriguez-Nava, V., Blaha, D., Winiarski, T., Mermillod-Blondin, F., & Cournoyer, B. (2020). Coalescence of bacterial groups originating from urban runoffs and artificial infiltration systems among aquifer microbiomes. Hydrology and Earth System Sciences, 24(9), 4257-4273. https://doi.org/10.5194/hess-24-4257-2020

Colinon, C., Jocktane, D., Brothier, E., Rossolini, G. M., Cournoyer, B., & Nazaret, S. (2010). Genetic analyses of Pseudomonas aeruginosa isolated from healthy captive snakes : Evidence of high inter- and intrasite dissemination and occurrence of antibiotic resistance genes. Environmental Microbiology, 12(3), 716-729. https://doi.org/10.1111/j.1462-2920.2009.02115.x

Collins, A. L., Pulley, S., Foster, I. D. L., Gellis, A., Porto, P., & Horowitz, A. J. (2017). Sediment source fingerprinting as an aid to catchment management : A review of the current state of knowledge and a methodological decision-tree for end-users. Journal of Environmental Management, 194, 86-108. https://doi.org/10.1016/j.jenvman.2016.09.075

Collins, A. L., Walling, D. E., & Leeks, G. J. L. (1997). Use of the geochemical record preserved in floodplain deposits to reconstruct recent changes in river basin sediment sources. Geomorphology, 19(1), 151-167. https://doi.org/10.1016/S0169-555X(96)00044-X

Cooper, D. M., Jenkins, A., Skeffington, R., & Gannon, B. (2000). Catchment-scale simulation of stream water chemistry by spatial mixing : Theory and application. Journal of Hydrology, 233(1-4), 121-137. https://doi.org/10.1016/S0022-1694(00)00230-4

David, L., Elmi, S., & Féraud, J. (1979). Carte géologique de la france au 1/50 000—Lyon. Feuille XXX-31. BRGM, Service Géologique National, 41.

https://doi.org/10.5194/egusphere-2025-2234
Preprint. Discussion started: 3 June 2025

Deletic, A., & Orr, D. W. (2005). Pollution buildup on road surfaces. Journal of Environmental Engineering, 131(1), 49-59. https://doi.org/10.1061/(ASCE)0733-9372(2005)131:1(49)

Delfour, J., Dufour, E., Feybesse, J. I., Johan, V., Kerrien, Y., Lardeaux, J. M., Lemière, B., Mouterde, R., & Tegyey, M. (1989). Notice explicative, carte géol. France (1/50000), feuille tarare (697). Orléans: Bureau de recherches géologiques et minières, 120.

Dembélé, A., Becouze-Lareure, C., Bertrand-Krajewski, J.-L., Barillon, B., Coquery, M., & Cren-Olivé, C. (2008). Prototype de collecte des retombées atmosphériques sèches et humides : Description du dispositif, mode de fonctionnement et premiers résultats pour les métaux dissous. In E. Berthier, G. Marie-Christine, J. Sage, & M. Seidl (Éds.), Actes des 8ième Journées doctorales en hydrologieurbaine (JDHU 2018) du 7 au 9 novembre 2019 à Paris,France.

Dunn, O. J. (1964). Multiple comparisons using rank sums. Technometrics : a journal of statistics for the physical, chemical, and engineering sciences, 6(3), 241-252. https://doi.org/10.2307/1266041

El Azzi, D., Probst, J. L., Teisserenc, R., Merlina, G., Baqué, D., Julien, F., Payre-Suc, V., & Guiresse, M. (2016). Trace element and pesticide dynamics during a flood event in the save agricultural watershed : Soil-river transfer pathways and controlling factors. Water, Air, and Soil Pollution, 227(12). https://doi.org/10.1007/s11270-016-3144-0

Eme, C., & Boutin, C. (2015). Composition des eaux usées domestiques par source d'émission à l'échelle de l'habitation. Etude bibliographique (p. 90) [Research Report]. irstea. https://hal.inrae.fr/hal-02605815

Fröhlich, H. L., Breuer, L., Frede, H.-G., Huisman, J. A., & Vaché, K. B. (2008). Water source characterization through spatiotemporal patterns of major, minor and trace element stream concentrations in a complex, mesoscale German catchment. Hydrological Processes, 22(12), 2028-2043. https://doi.org/10.1002/hyp.6804

Fröhlich, H. L., Breuer, L., Vaché, K. B., & Frede, H.-G. (2008). Inferring the effect of catchment complexity on mesoscale hydrologic response. Water Resources Research, 44(9). https://doi.org/10.1029/2007WR006207

Giri, S., & Qiu, Z. (2016). Understanding the relationship of land uses and water quality in Twenty First Century : A review. Journal of Environmental Management, 173, 41-48. https://doi.org/10.1016/j.jenvman.2016.02.029

Gnouma, R. (2006). Aide à la calibration d'un modèle hydrologique distribué au moyen d'une analyse des processus hydrologiques : Application au bassin versant de l'Yzeron (p. 412) [Phd, Thèse de doctorat, INSA Lyon]. https://hal.inrae.fr/tel-02588466

Gonzales, A. L., Nonner, J., Heijkers, J., & Uhlenbrook, S. (2009). Comparison of different base flow separation methods in a lowland catchment. Hydrology and Earth System Sciences, 13(11), 2055-2068. https://doi.org/10.5194/hess-13-2055-2009

Goutaland, D. (2009). Programme ANR AVuPUR - Prospection géophysique par panneau éléctrique de trois parcelles d'un sous-bassin versant de l'Yzeron. CETE de Lyon.

Grandjouan, O. (2024). Apports de la biogéochimie pour l'évaluation d'un modèle hydrologique distribué en milieu péri-urbain [Phd]. Thèse de doctorat, INRAE.

Grandjouan, O., Branger, F., Masson, M., Cournoyer, B., & Coquery, M. (2023). Identification and estimation of hydrological contributions in a mixed land-use catchment based on a simple biogeochemical and hydro-meteorological dataset. Hydrological Processes, 37(12), e15035. https://doi.org/10.1002/hyp.15035

Helms, J. R., Stubbins, A., Ritchie, J. D., Minor, E. C., Kieber, D. J., & Mopper, K. (2008). Absorption spectral slopes and slope ratios as indicators of molecular weight, source, and photobleaching of chromophoric dissolved organic matter. Limnology and Oceanography, 53(3), 955-969. https://doi.org/10.4319/lo.2008.53.3.0955

Iorgulescu, I., Beven, K. J., & Musy, A. (2005). Data-based modelling of runoff and chemical tracer concentrations in the Haute-Mentue research catchment (Switzerland). Hydrological Processes, 19(13), 2557-2573. https://doi.org/10.1002/hyp.5731

Jacqueminet, C., Kermadi, S., Michel, K., Béal, D., Gagnage, M., Branger, F., Jankowfsky, S., & Braud, I. (2013). Land cover mapping using aerial and VHR satellite images for distributed hydrological modelling of periurban catchments : Application to the Yzeron catchment (Lyon, France). Journal of Hydrology, 485, 68-83. https://doi.org/10.1016/j.jhydrol.2013.01.028

Jankowfsky, S. (2011). Understanding and modelling of hydrological processes in small peri-urban catchments using an object-oriented and modular distributed approach Application to the Chaudanne and Mercier sub-catchments

(Yzeron catchment, France) (p. 331) [Theses, Thèse de doctorat, spécialité Océan, Atmosphère, Hydrologie, Ecole Doctorale Terre Univers Environnement, Université de Grenoble]. https://hal.inrae.fr/tel-02596792

Kruskal, W. H., & Wallis, W. A. (1952). Use of ranks in one-criterion variance analysis. Journal of the American Statistical Association, 47(260), 583-621. https://doi.org/10.2307/2280779

Kuhlemann, L.-M., Tetzlaff, D., & Soulsby, C. (2021). Spatio-temporal variations in stable isotopes in peri-urban catchments : A preliminary assessment of potential and challenges in assessing streamflow sources. Journal of Hydrology, 600, 126685. https://doi.org/10.1016/j.jhydrol.2021.126685

Labbas, M. (2014). Modélisation hydrologique de bassins versants périurbains et influence de l'occupation du sol et de la gestion des eaux pluviales. Application au bassin de l'Yzeron (130 km2) [Phd]. Thèse de doctorat, Université Grenoble Alpes.

Lachassagne, P., Dewandel, B., & Wyns, R. (2021). Review : Hydrogeology of weathered crystalline/hard-rock aquifers—guidelines for the operational survey and management of their groundwater resources. Hydrogeology Journal, 29(8), 2561-2594. https://doi.org/10.1007/s10040-021-02339-7

Ladouche, B., Probst, A., Viville, D., Idir, S., Baqué, D., Loubet, M., Probst, J.-L., & Bariac, T. (2001). Hydrograph separation using isotopic, chemical and hydrological approaches (Strengbach catchment, France). Journal of Hydrology, 242(3-4), 255-274. https://doi.org/10.1016/S0022-1694(00)00391-7

Lafont, M., Vivier, A., Nogueira, S., Namour, P., & Breil, P. (2006). Surface and hyporheic oligochaete assemblages in a french suburban stream. Hydrobiologia, 564(1), 183-193. https://doi.org/10.1007/s10750-005-1718-8

Lagouy, M., Branger, F., & Breil, P. (2022). Rainfall monitoring on the Yzeron catchment since 1997 [Jeu de données]. Recherche Data Gouv. https://doi.org/10.57745/VVQ2X9

Lamprea, K., & Ruban, V. (2011). Pollutant concentrations and fluxes in both stormwater and wastewater at the outlet of two urban watersheds in Nantes (France). Urban Water Journal, 8(4), 219-231. https://doi.org/10.1080/1573062X.2011.596211

Langlois, J. L., & Mehuys, G. R. (2003). Intra-storm study of solute chemical composition of overland flow water in two agricultural fields. Journal of Environmental Quality, 32(6), 2301-2310. https://doi.org/10.2134/jeq2003.2301

Li, P., & Hur, J. (2017). Utilization of UV-Vis spectroscopy and related data analyses for dissolved organic matter (DOM) studies : A review. Critical Reviews in Environmental Science and Technology, 47(3), 131-154. https://doi.org/10.1080/10643389.2017.1309186

Lin, B., An, X., Zhao, C., Gao, Y., Liu, Y., Qiu, B., Qi, F., & Sun, D. (2024). Analysis of urban composite non-point source pollution characteristics and its contribution to river DOM based on EEMs and FT-ICR MS. Water Research, 266, 122406. https://doi.org/10.1016/j.watres.2024.122406

Liu, W.-R., Zeng, D., She, L., Su, W.-X., He, D.-C., Wu, G.-Y., Ma, X.-R., Jiang, S., Jiang, C.-H., & Ying, G.-G. (2020). Comparisons of pollution characteristics, emission situations, and mass loads for heavy metals in the manures of different livestock and poultry in China. In Science of the Total Environment (Vol. 734). https://doi.org/10.1016/j.scitotenv.2020.139023

Liu, Y., Walling, D. E., Yang, M., & Zhang, F. (2023). Sediment source fingerprinting and the temporal variability of source contributions. Journal of Environmental Management, 338, 117835. https://doi.org/10.1016/j.jenvman.2023.117835

Madani, E. M., Jansson, P. E., & Babelon, I. (2017). Differences in water balance between grassland and forest watersheds using long-term data, derived using the CoupModel. Hydrology Research, 49(1), 72-89. https://doi.org/10.2166/nh.2017.154

Marti, R., Ribun, S., Aubin, J.-B., Colinon, C., Petit, S., Marjolet, L., Gourmelon, M., Schmitt, L., Breil, P., Cottet, M., & Cournoyer, B. (2017). Human-driven microbiological contamination of benthic and hyporheic sediments of an intermittent peri-urban river assessed from MST and 16S rRNA genetic structure analyses. Frontiers in Microbiology, 8, 19. https://doi.org/10.3389/fmicb.2017.00019

Martins, J., Coquery, M., Robinet, N., Nord, G., Duwig, C., Legout, C., Morel, M. C., Spadini, L., Hachgenei, N., Némery, J., Mao, P., Margoum, C., Miege, C., Daval, A., Mathon, B., & Liger, L. (2019). Origine et devenir des contaminants PHARMAceutiques dans les Bassins Versants agricoles. Le cas de la Claduègne (Ardèche). PHARMA-BV (p. 2). https://hal.inrae.fr/hal-02609731

Marx, C., Tetzlaff, D., Hinkelmann, R., & Soulsby, C. (2021). Isotope hydrology and water sources in a heavily urbanized stream. Hydrological Processes, 35(10), e14377. https://doi.org/10.1002/hyp.14377

https://doi.org/10.5194/egusphere-2025-2234
Preprint. Discussion started: 3 June 2025

McElmurry, S. P., Long, D. T., & Voice, T. C. (2014). Stormwater dissolved organic matter : Influence of land cover and environmental factors. Environmental Science and Technology, 48(1), 45-53. https://doi.org/10.1021/es402664t

Mejía, A. I., & Moglen, G. E. (2010). Impact of the spatial distribution of imperviousness on the hydrologic response of an urbanizing basin. Hydrological Processes, 24(23), 3359-3373. https://doi.org/10.1002/hyp.7755

Nguyen, H., Peche, A., & Venohr, M. (2021). Modelling Of Sewer Exfiltration To Groundwater In Urban Wastewater Systems : A Critical Review. Journal of Hydrology, 126130. https://doi.org/10.1016/j.jhydrol.2021.126130

Penuelas, J., Coello, F., & Sardans, J. (2023). A better use of fertilizers is needed for global food security and environmental sustainability. Agriculture & Food Security, 12(1), 5. https://doi.org/10.1186/s40066-023-00409-5

Peuravuori, J., & Pihlaja, K. (1997). Molecular size distribution and spectroscopic properties of aquatic humic substances. Analytica Chimica Acta, 337(2), 133-149. https://doi.org/10.1016/S0003-2670(96)00412-6

Pozzi, A. C. M., Petit, S., Marjolet, L., Youenou, B., Lagouy, M., Namour, P., Schmitt, L., Navratil, O., Breil, P., Branger, F., & Cournoyer, B. (2024). Ecological assessment of combined sewer overflow management practices through the analysis of benthic and hyporheic sediment bacterial assemblages from an intermittent stream. Science of The Total Environment, 907, 167854. https://doi.org/10.1016/j.scitotenv.2023.167854

Ramon, R. (2021). Quantifying sediment source contributions in contrasted agricultural catchments (Uruguay River, Southern Brazil) (Theses 2021UPASJ009, Thèse de doctorat, Université Paris-Saclay ; Universidade Federal do Rio Grande do Sul (Porto Alegre, Brésil)). https://theses.hal.science/tel-03434617

Sanisaca, L. E. G., Gellis, A. C., & Lorenz, D. L. (2017). Determining the sources of fine-grained sediment using the Sediment Source Assessment Tool (Sed_SAT). In Open-File Report (p. 116). https://doi.org/10.3133/ofr20171062

Shi, M.-M., Wang, X.-M., Chen, Q., Han, B.-H., Zhou, B.-R., Xiao, J.-S., & Xiao, H.-B. (2021). Responses of soil moisture to precipitation and infiltration in dry and wet alpine grassland ecosystems. In Acta Prataculturae Sinica (Vol. 30, Numéro 12, p. 49-58). https://doi.org/10.11686/cyxb2020436

Singh, S. K., & Stenger, R. (2018). Indirect methods to elucidate water flows and contaminant transfer pathways through meso-scale catchments – A review. Environmental Processes, 5(4), 683-706. https://doi.org/10.1007/s40710-018-0331-6

Stock, B. C., Jackson, A. L., Ward, E. J., Parnell, A. C., Phillips, D. L., & Semmens, B. X. (2018). Analyzing mixing systems using a new generation of Bayesian tracer mixing models. PeerJ, 6(e5096).

Sun, Z.-X., Cui, J.-F., Cheng, J.-H., & Tang, X.-Y. (2024). A novel tool for tracing water sources of streamflow in a mixed land-use catchment. Science of The Total Environment, 912, 168800. https://doi.org/10.1016/j.scitotenv.2023.168800

Tardy, Y., Bustillo, V., & Boeglin, J.-L. (2004). Geochemistry applied to the watershed survey : Hydrograph separation, erosion and soil dynamics. A case study : The basin of the Niger River, Africa. Applied Geochemistry, 19(4), 469-518. https://doi.org/10.1016/j.apgeochem.2003.07.003

Tiecher, T., Caner, L., Minella, J. P. G., & dos Santos, D. R. (2015). Combining visible-based-color parameters and geochemical tracers to improve sediment source discrimination and apportionment. Science of The Total Environment, 527-528, 135-149. https://doi.org/10.1016/j.scitotenv.2015.04.103

Tran, N. H., Reinhard, M., Khan, E., Chen, H., Nguyen, V. T., Li, Y., Goh, S. G., Nguyen, Q. B., Saeidi, N., & Gin, K. Y.-H. (2019). Emerging contaminants in wastewater, stormwater runoff, and surface water : Application as chemical markers for diffuse sources. Science of The Total Environment, 676, 252-267. https://doi.org/10.1016/j.scitotenv.2019.04.160

Tromp-van Meerveld, H. J., & McDonnell, J. (2006). Threshold relations in subsurface stormflow : 2. The fill and spill hypothesis. Water Resources Research, 42(2). https://doi.org/10.1029/2004WR003800

Uber, M., Legout, C., Nord, G., Crouzet, C., Demory, F., & Poulenard, J. (2019). Comparing alternative tracing measurements and mixing models to fingerprint suspended sediment sources in a mesoscale Mediterranean catchment. Journal of Soils and Sediments, 19(9), 3255-3273. https://doi.org/10.1007/s11368-019-02270-1

Walsh, C. J., Roy, A. H., Feminella, J. W., Cottingham, P. D., Groffman, P. M., & Morgan, R. P. (2005). The urban stream syndrome : Current knowledge and the search for a cure. Journal of the North American Benthological Society, 24(3), 706-723. https://doi.org/10.1899/04-028.1

https://doi.org/10.5194/egusphere-2025-2234
Preprint. Discussion started: 3 June 2025

881 Wang, Y.-H., Zhang, P., He, C., Yu, J.-C., Shi, Q., Dahlgren, R. A., Spencer, R. G. M., Yang, Z.-B., & Wang, J.-J. (2023).
882 Molecular signatures of soil-derived dissolved organic matter constrained by mineral weathering. Fundamental
883 Research, 3(3), 377-383. https://doi.org/10.1016/j.fmre.2022.01.032
884 Wilkinson, S. N., Hancock, G. J., Bartley, R., Hawdon, A. A., & Keen, R. J. (2013). Using sediment tracing to assess
885 processes and spatial patterns of erosion in grazed rangelands, Burdekin River basin, Australia. Agriculture,
886 Ecosystems and Environment, 180, 90-102. https://doi.org/10.1016/j.agee.2012.02.002
887